Large-scale template-based structural modeling of T-cell receptors with known antigen specificity reveals complementarity features.

Dmitrii S. Shcherbinin[1,2], Vadim K. Karnaukhov[3], Ivan V. Zvyagin[4], Dmitriy M. Chudakov[1,3,4], Mikhail Shugay[1,4,*]

1. Institute of Translational Medicine, Center for Precision Genome Editing and Genetic Technologies for Biomedicine, Pirogov Russian National Research Medical University, Moscow, Russia
2. Institute of Biomedical Chemistry, Moscow, Russia
3. Center of Life Sciences, Skolkovo Institute of Science and Technology, Moscow, Russia
4 .Shemyakin-Ovchinnikov Institute of Bioorganic Chemistry, Russian Academy of Sciences, Moscow, Russia

** - to whom correspondence should be addressed, mikhail.shugay@gmail.com*

Abstract. T-cell receptor (TCR) recognition of foreign peptides presented by the major histocompatibility complex (MHC) initiates the adaptive immune response against pathogens. A large number of TCR sequences specific to different antigens are known to date, however, the structural data describing the conformation and contacting residues for TCR:antigen:MHC complexes is relatively limited. In the present study we aim to extend and analyze the set of available structures by performing highly accurate template-based modeling of TCR:antigen:MHC complexes using TCR sequences with known specificity. Using the set of 29 complex templates and 732 specificity records, we built a database of 1517 model structures. This database allowed us to analyze features of amino acid contacts in TCR:antigen interfaces that govern antigen recognition preferences and interpret these interactions in terms of physicochemical properties of interacting residues. Our results provide a methodology for building high-quality TCR:antigen:MHC models for certain antigens that can be utilized to assay TCR specificity.

Introduction

Specific interaction between T-cell receptors (TCRs) and major histocompatibility complex (MHC)-peptide complexes is a key initiation factor of adaptive immunity-driven physiological processes *(1)* that happens upon recognition of an infected or antigen-presenting cell by cognate T-cell. TCR molecules are heterodimers whose genes are formed via the process of V(D)J-rearrangement that ensures the presence of a great diversity of TCR sequences in an individual, required to recognize and target previously unencountered pathogens viewed through the lens of MHC molecules presenting peptides *(2,3)*. Describing molecular mechanisms governing antigen recognition is therefore the cornerstone of adaptive immunity

studies making it possible to predict immune responses to specific antigens, as well as cross-reactivity and selectivity of TCRs in the near future *(4)*.

Currently, several databases gathering experimental information about selective recognition of TCR, peptide and MHC sequences are available to the research community: VDJdb, IEDB, McPAS-TCR *(5–7)*. These resources store and aggregate data on primary TCR sequences, cognate epitopes and MHC context mined using literature search.

In addition there are more than 280 crystal structures stored in the Protein Data Bank (PDB) that encode the geometry and physical contacts in TCR-pMHC complexes *(8,9)*. Several computational approaches have been developed for homology-based modeling of individual TCR structures or TCRs in their triple complex with peptide-MHC molecules they recognize. Promising software tools and approaches in this area include the TCRmodel (10) and TCR-pMHC-models *(11)* services.

In addition to homology modeling approaches, it has been shown that AlphaFold software, which is based on deep learning techniques and has revolutionized the field of protein structure prediction, can be used for the *de-novo* modeling of TCR complexes with pMHC, although the proposed pipeline needs further tuning *(12)*.

Recent research studies, focused on structural bioinformatics and molecular modeling of TCR-epitope-MHC complexes, can be categorized into two primary areas of study. The first area involves large-scale modeling approaches and mathematical modeling of a significant amount of structural data, while the second area is devoted to a detailed examination of individual complexes and enhancing the precision of evaluating binding specificity and affinity.

Large-scale attempts to model multiple TCR:pMHC complexes have been carried out in a number of studies discussed further. Most of these works were focused on serving as a proof-of-concept and as a benchmark for modeling software, not directly aimed at general applications, such as studying regularities in TCR:pMHC recognition at the residue level or imputing a missing TCR:pMHC structure for a TCR linked to a certain disease. A consistent database of over 23,000 TCR complex structures with pMHC was created using template-based approaches for TCR (Repertoire Builder *(13)*, LYRA *(14)*), MHC (NetMHCpan *(15)*) modeling, and construction of docked complexes *(16)*.

Machine learning algorithms have demonstrated their usefulness in predicting TCR-peptide interactions employing high similarity (HS) and random sampling strategies for deep learning models *(17)* and evaluating binding affinity by training a random forest classifier model using the ATLAS database *(18)*.

On the other hand, it was demonstrated using two contrasting TCR−pHLA test sets that the MMPB/GBSA approach can be effectively applied during the binding affinity calculation. However, the protocol needs to be adjusted based on the similarity of the compared structures (19). Analysis of multiple molecular docking approaches *(20)* and their corresponding scoring functions has indicated that hydrophobic and electrostatic interactions play key roles in TCR-pMHC recognition. Additionally, highlighting of contacting residues of TCR and peptide has been shown to improve modeling of the whole complex, as well as flexible CDR3 loops.

The importance of hydrophobic interactions and pi-stacking forces in TCR contacts with HLA-A*02-restricted peptides, was also analyzed and illustrated using molecular dynamics simulations and binding free energy calculations *(21)*.

Despite the fact that much attention has been paid to the study of SARS-CoV2 recently, only a few COVID-associated TCRs have a resolved TCR:pMHC structure to date *(22–25)*. Having a variety of structures with SARS-CoV-2 epitopes can aid in studying T-cell recognition of infected cells, especially since the number of known COVID-associated TCRs is constantly growing *(5)*.The study of TCR – peptide MHC complexes is important in understanding the immune response to SARS-CoV-2 vaccinations and the viral immune evasion strategies employed by VOCs (Variants of concern). Mutations in T cell epitopes can disrupt recognition by TCRs, which highlights the importance of modeling and studying the spatial structures of TCR – peptide MHC complexes.

There are several main factors that guide antigen recognition in TCR:pMHC complex: placement of the peptide in the MHC groove, pairing of TCR- alpha and beta chains, specific orientation of pMHC complex against T-cell receptor and selective interaction of TCR residues with MHC and peptide.

Most studies suggest that TCRs recognize peptide-MHC complexes via CDR1-3 loops. While CDR1 and CDR2 loops stabilize binding with MHC molecules and target small parts of a protein, most of the interaction between TCR and antigen occurs via CDR3, which are omega-loops of 10-20 amino acids *(26,27)*. Also, it has been shown that CDR3 loop sequence's mid-region creates most of contacts with peptide due to the loop and peptide geometry. Additionally, both alpha and beta chains contribute to antigen recognition, although sometimes this contribution is disproportionate *(28)*.

The present study reports the results of large-scale template-based modeling of the VDJdb, which is a curated database of TCR sequences with known specificities. Our primary aim is to establish a pipeline that can be easily employed to create accurate and reliable spatial structures for studies that report massive sequencing of TCRs specific to a panel of antigens. By applying this pipeline to the existing database we aim at providing access to structural data for immunologists and biologists unfamiliar with *in silico* structural modeling. We also demonstrate, as a proof-of-concept, that such modeling can be used to study features of residue interactions in TCR:pMHC complexes, and report statistics of various physicochemical interactions between TCR and peptide.

Results

Building a compendium of TCR:pMHC models for VDJdb

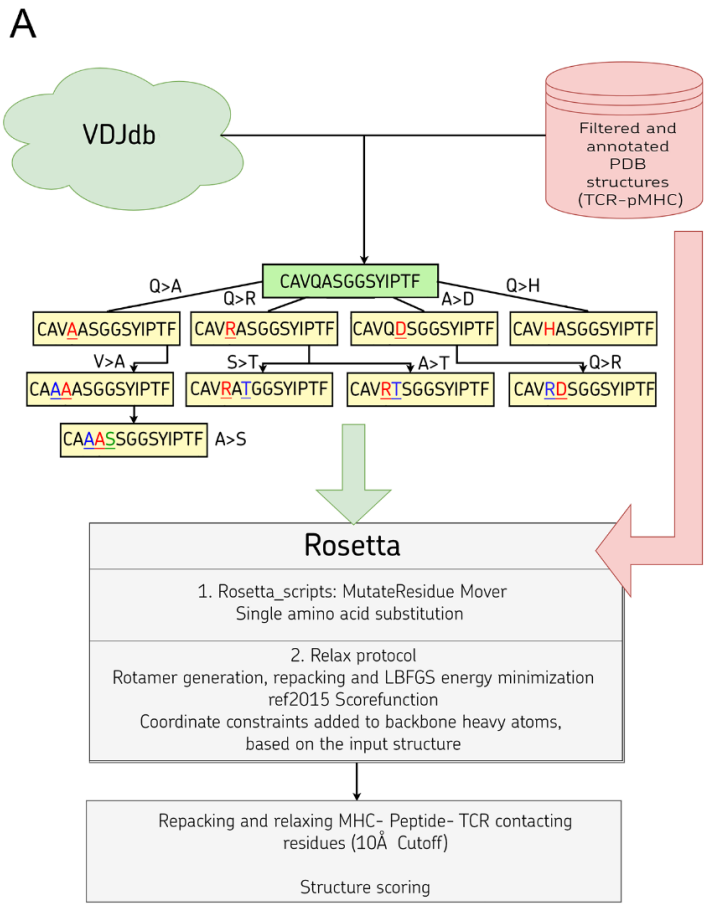
A
VDJdb
Filtered and annotated PDB structures (TCR-pMHC)
CAVQASGGSYIPTF
Q>A
Q>R
A>D
Q>H
CAVAASGGSYIPTF
CAVRASGGSYIPTF
CAVQDSGGSYIPTF
CAVHASGGSYIPTF
V>A
S>T
A>T
Q>R
CAAAASGGSYIPTF
CAVRATGGSYIPTF
CAVRTSGGSYIPTF
CAVRDSGGSYIPTF
CAAASSGGSYIPTF
A>S
Rosetta
1. Rosetta_scripts: MutateResidue Mover
Single amino acid substitution
2. Relax protocol
Rotamer generation, repacking and LBFGS energy minimization
ref2015 Scorefunction
Coordinate constraints added to backbone heavy atoms,
based on the input structure
Repacking and relaxing MHC- Peptide- TCR contacting residues (10Å Cutoff)
Structure scoring

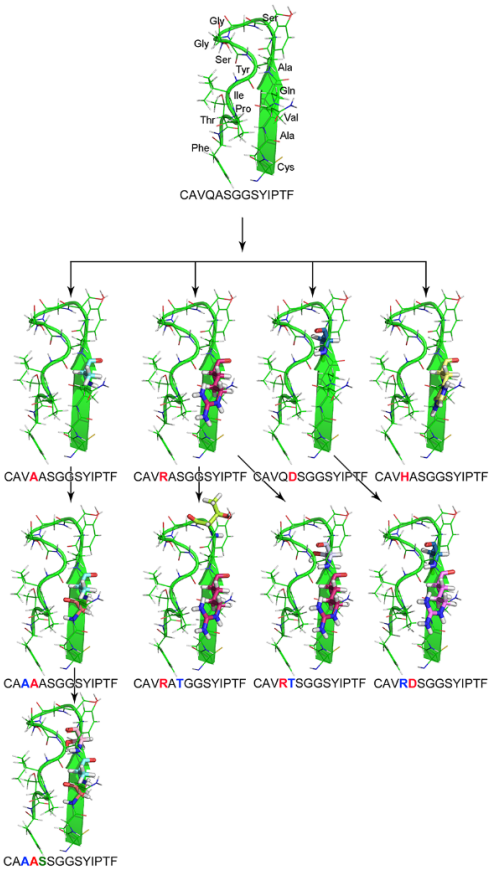
B
CAVQASGGSYIPTF
CAVAASGGSYIPTF
CAVRASGGSYIPTF
CAVQDSGGSYIPTF
CAVHASGGSYIPTF
CAAAASGGSYIPTF
CAVRATGGSYIPTF
CAVRTSGGSYIPTF
CAVRDSGGSYIPTF
CAAASSGGSYIPTF

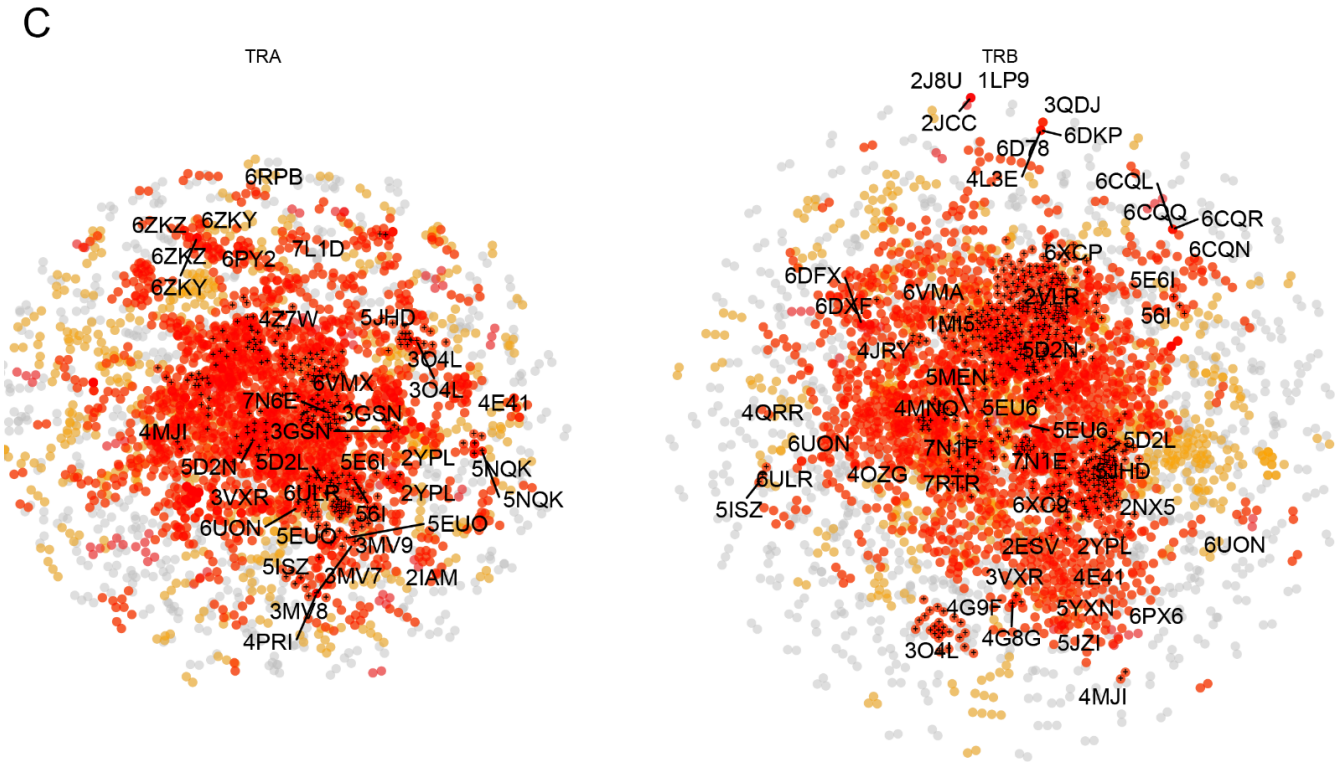
C
TRA
6RPB
6ZKZ
6ZKY
6PY2
7L1D
4Z7W
5JHD
3O4L
6VMX
7N6E
3GSN
4E41
4MJI
5D2N
5D2L
5E6I
2YPL
5NQK
3VXR
6ULR
56I
6UON
5EUO
3MV9
5ISZ
3MV7
2IAM
3MV8
4PRI
TRB
2J8U
1LP9
2JCC
3QDJ
6DKP
6D78
4L3E
6CQL
6CQQ
6CQR
6CQN
6XCP
6DFX
6DXF
6VMA
2VLR
5E6I
1MI5
4JRY
5D2N
5MEN
4QRR
4MNQ
5EU6
6UON
7N1F
7N1E
6UHD
4OZG
7RTR
5ISZ
6XQ9
2NX5
2ESV
2YPL
3VXR
4E41
4G9F
5YXN
6PX6
3O4L
4G8G
5JZI
4MJI

Figure 1. *A) Pipeline used in the stepwise amino acid mutation modeling approach applied in present study. B) Mutation path in one of the studied CDR3 clusters starting from a known PDB structure carrying CAVQASGGSYIPTF CDR3α loop. 2NX5 PDB structure (29) was used as the initial template. C) CDR3 sequence similarity map of VDJdb, layout of a graph with edges connecting CDR3 sequences that differ by no more than a single amino acid mismatch. CDR3 sequences having PDB templates are shown with text. Orange points show VDJdb entries that were classified as belonging to a sequence homology motif (described in (30)), red points are neighbors (connected by no more than 3 subsequent amino acid substitutions) of PDB templates modeled in present study.*

In this study we developed an approach for modeling T cell receptor CDR3 loops by stepwise introduction of single amino acid mutations to known spatial structures of complexes, applied it to 29 templates and analyzed contacting residues between CDR3 loops and peptides in modeled complexes.

The pipeline of our approach is shown in **Figure 1 (A** and **B)**. In the first step we created a filtered and annotated database of TCR-pMHC PDB structures and built clusters of CDR3 sequences, using CDR3 loops from known PDBs as cores and annotated sequences from VDJdb. In the next stage we calculated pathways for the sequential introduction of single amino acid substitutions to cover all sequences in selected clusters, starting from known PDB structures. The actual extent of VDJdb coverage by our modeling approach is depicted in **Figure 1C**, and the modeling paths are presented in **Supplementary Figure S1**.

Using 1030 unique pathways, all initial structures were mutated and further optimized using Rosetta protocols. As a result, we built 1517 models based on 29 template structures from the PDB database, which contain 247 unique sequences of CDR3 loops for TCR-alpha and 485 for TCR-beta chains. All modeled CDR3 sequences are presented in **Supplementary Figure S2**, and the number of models according to TCR chains, presence of contact with peptide, and type of contact are presented in **Supplementary Table S1**.

The initial templates are presented in **Table1**. It is worth noting that some PDB templates carried identical TCR chains, peptides and MHC molecules. During further analysis, models built based on such templates were grouped, and their calculated spatial and energy properties were averaged. These grouped structures would be referred to as “merged”.

Analysis of CDR3:peptide contacts in modeled structures

Using a 5Å cutoff distance, close-contacting (or “interacting”) residues of “mutated” CDR3 loops and peptides were identified in all modeled structures. It was shown that only about half of them carried substitution in close-contacting positions: approximately 49% (742 models out of 1517) in all TCR-pMHC complex models and ~54% (561 models out of 1030) in “merged” structures.

Since all the studied CDR3 loops were selected from the database of experimentally determined sequences of recognizable TCR, peptides and MHC molecules, modeled amino

acid substitutions should not dramatically influence the binding between T-cell receptors and epitopes. That might be the reason why many amino acid variations were substituted in non-contacting positions - they are simply distal and do not alter TCR-pMHC interface. Additionally, it can be assumed that the remaining substitutions in close-contacting positions should not be critical for the affinity level of binding between CDR3 loops and epitopes.

CDR3 – epitope interactions were analyzed in all initial templates, and for each structure the most valuable positions in CDR3 loops were identified according to the most significant energetic impact of corresponding amino acids on TCR-epitope binding. These results were compared with estimated frequencies of amino acid variations in each position on CDR3 loops in our modeled structures. It was found out that only 11% of all mutations and 23% of mutations in contacting residues were in energetically valuable positions. After merging close and identical structures, the rate slightly increased to 15% and 27% respectively. These results also indicate that substitutions mainly occur in regions of CDR3 loops that are not very important for epitope recognition, thus preserving specificity and affinity of binding in TCR -pMHC complexes.

All amino acid pairs involved in CDR3 - peptide interactions were identified and counted in all modeled and 152 original structures of human TCR-peptide-MHCI complexes. Interactions between amino acid residues of CDR3 loops and peptides were classified based on their distances and contacting parts: main chain or side chain groups. Four groups were formed based on these parameters: (1) all contacting residue pairs, (2) closest contacting residues, (3) residues contacting through side chain groups, and (4) closest contacting residues through side chain groups. Since contacting residues were identified using only a cutoff distance, a single residue of CDR3 loop may interact with multiple residues of peptide. The first group of contacts included all found pairs of CDR3 - peptide residues that were within 5Å of each other. The second group included specific residues of CDR3 loops and the closest residues of peptide. The third and fourth groups were gathered based on a similar idea, but in addition to the distance, type of interaction was also taken into account: at least one of the residues in a pair must interact through a side chain group. Analysis of side chain groups is crucial because practically all physicochemical features of amino acid residues are “encoded” in side chain groups.

The number of all found contacting amino acid pairs between CDR3 loops and peptides in original and modeled structures is presented in **Figure 2**.

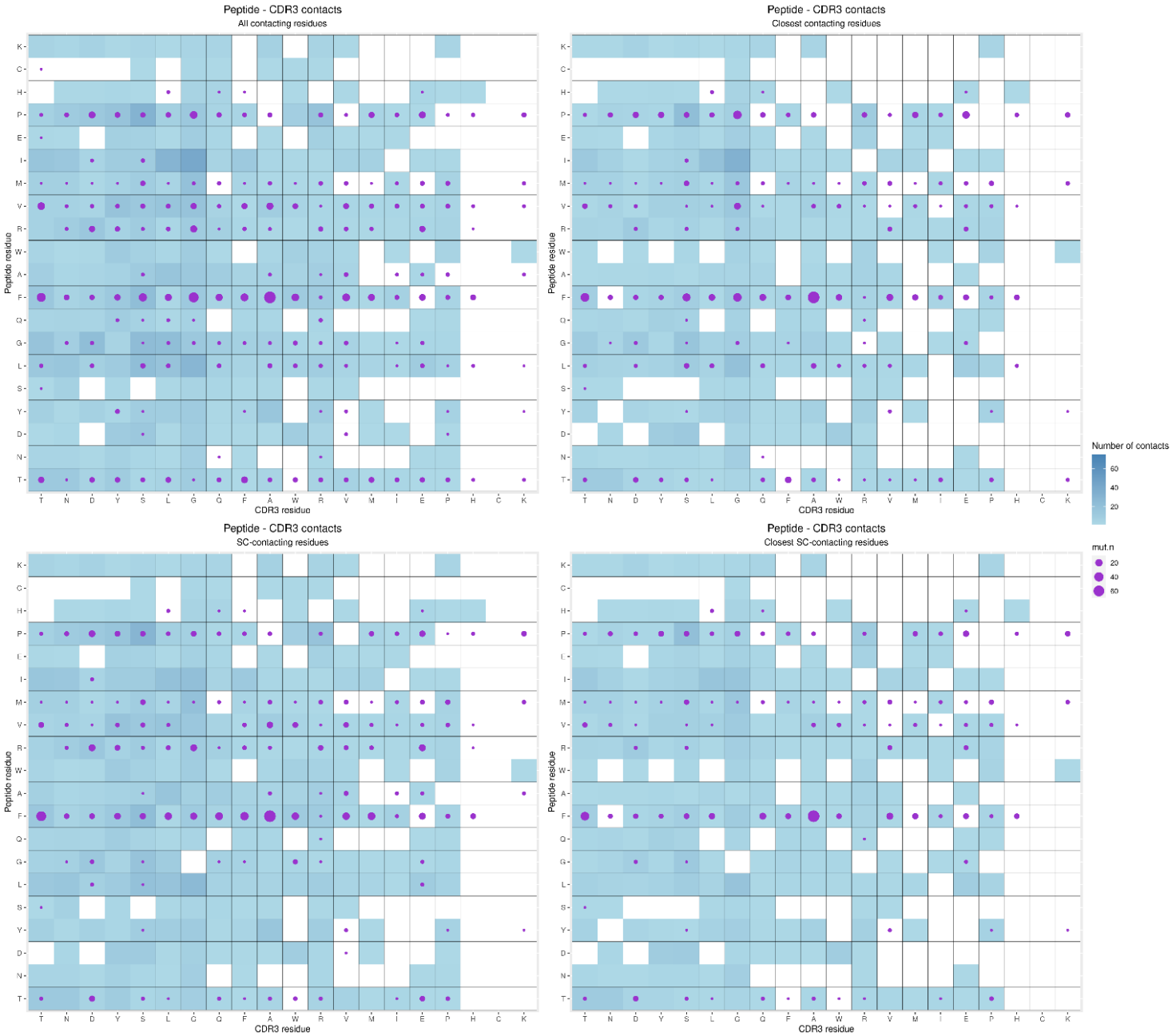

Figure 2. Contacting amino acid pairs identified in original and modeled structures. *Contacts in original structures are represented as squares, and contacts in modeled structures are represented as circles. The number of identified contacting pairs is illustrated as a gradient fill for original structures, and the size of circles represents the results for modeled structures. The results for all contacting residue pairs are presented in the upper-left corner; closest contacting residue pairs are shown in the upper right corner. Amino acid residues, contacted by at least one side chain group are in the down-left corner, and the results for closest amino acid residues contacting by at least one side chain group are presented in the down-right corner.*

It can be seen that, even though there are some new contacting residue pairs in the modeled structures that were not found in the original structures, the majority was not unique.

Correlation of CDR3:peptide binding energy values and amino acid properties

It was previously shown *(31)* that the most important energy terms during the calculation of free binding energies between TCRs and peptides were the attractive van der Waals impact energy, solvation energy, and side-chain – side-chain hydrogen bond energy, while the repulsive van der Waals term was insignificant. Thus, in our research, energy values for contacting residues and interfaces between modified CDR3 loops and peptides in all modeled complexes were calculated using full Rosetta scoring functions and two of its limited variations: “Large patch” and “Small patch” presets. As all models were built using stepwise introduction of single amino acid substitutions, we calculated delta values of free energies of interacting interfaces between neighboring complexes. These energy values represent the impacts of point amino acid variations on the affinity of complexes. Henceforth that type of values would be referred to as “dEnergy”.

<u>Correlation between Blosum scores and dEnergy values</u>

Two types of Blosum matrices (Blosum62 and Blosum100) were used to study the consistency between amino acid substitution scores and their impact on dEnergy in modeled complexes. Pearson’s correlations were calculated between absolute values of free energy adjustments caused by mutation and one of three modified Blosum indices of corresponding substitutions: Clustered Target Frequencies (QIJ), Clustered Scoring Matrix in Bit Units (SIJ) or most commonly used Clustered Scoring Matrix in 1/2 Bit Units (BLA). Adjusted index values were calculated as follows:

$$\frac{Blos_i(substiution) - Blos_i(from) - Blos_i(to)}{2}$$

Where $Blos_i$(substitution)- Blosum index of studied substitution

$Blos_i$(from) - Blosum index of a match of origin residue

$Blos_i$(to)- Blosum index of a match of new residue

As Blosum scores represent the ratio of the likelihood of two amino acids being exchanged with biological significance, it is more reasonable to compare them with absolute values of dEnergy, and not real ones. Thus, we can evaluate the impact of exchanging close amino acid residues or more dissimilar ones. Energy values were calculated using the full Rosetta scoring function and two types of presets.

Correlations were analyzed for all mutated residues in CDR3 loops and separately for substitutions in only contacting positions. Top 20 corresponding correlation values and p-values are presented in **Table 2.**

It was observed that the correlations between different Blosum 62 or Blosum 100 indexes and absolute delta energy values were very poor overall. The best correlation was observed

between BLA.62 values and the absolute value of dEnergy, calculated using the “Small patch” preset in structures that carried mutations in contacting positions. Pearson correlation values (R coefficient) was -0.22 and -0.13 for minimized and repacked structures respectively. The results are presented in **Fig. 3**. It can also be observed that correlation is better for TCRβ chains, which corresponds to previously shown results that beta-chains are more crucial for the specificity of peptide recognition and binding.

These results show that standard Blosum matrices might not be as informative in the analysis of full CDR3 sequences, their clusterization and prediction of binding with specific peptides. Instead of aligning and analyzing full sequences in these approaches, special attention should be paid to contacting parts.

Despite the low correlations overall, it was mentioned that using energy minimization as the final optimization of models led to a slight improvement of corresponding values compared to repacking. This can be explained by the “fitting” of contacting interfaces in TCR-pMHC complexes after repacking of “mutated” models, which resulted in “smoothing” (reduction) of the substitution impact.

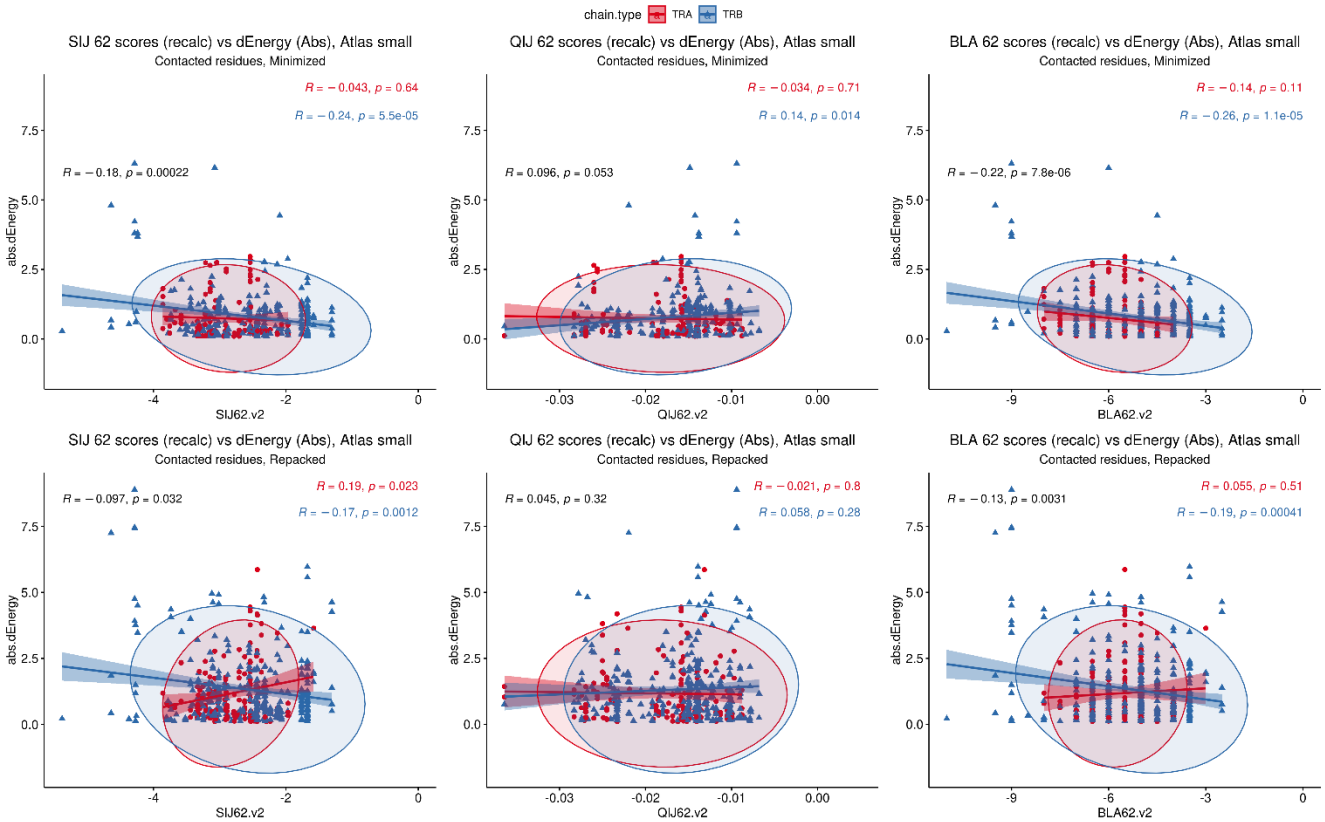

Figure. 3 Correlation of BLOSUM62 matrix indices and absolute values of dEnergy, calculated for modeled structures. Corresponding values for TCRa and TCRb are colored red and cyan.

Influence of remoteness of contacting amino acids on dEnergy

We additionally analyzed the impact of the distance between substituted residues and peptides on dEnergy of TCR-pMHC binding. As mutated residues in CDR3 can interact with more than one residue of epitope, we used minimal distance values in these cases. It was shown that the total Pearson correlation values between distance and absolute values of dEnergy in minimized modeled structures were -0.24, -0.38 and -0,4 for energy values calculated using the full Rosetta scoring function, “Large-“ and “Small patch” presets respectively. The negativity in correlation values indicates that the more distant a modeled substitution is, the less it impacts dEnergy values, which makes biophysical sense.

Analyzing these dependencies for TCRα and TCRβ separately, it can be seen that correlation was better for TCRβ in comparison with TCRα. These results indicate that CDR3 loops of beta-chains might have a greater impact on peptide recognition than TCR-alpha’s. Corresponding correlations, calculated for repacked structures were smaller: -0.034, -0.23 and -0.16. This decrease in correlation also supports the concept of “fitting” of mutated CDR3 residues after repacking optimization. Correlation graphs are presented in **Figure 4.**

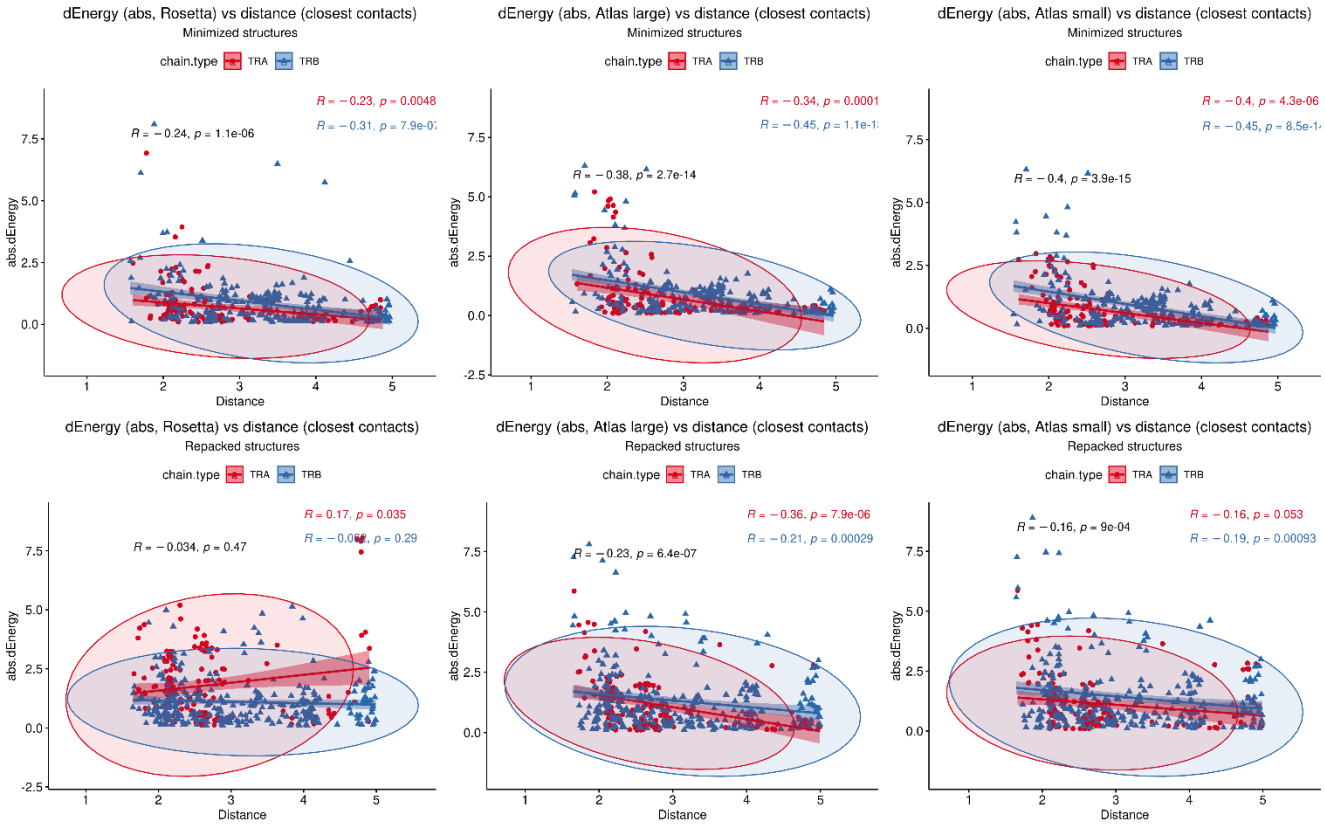

Figure 4. *Correlation between remoteness of contacting residues in CDR3-peptide interface and absolute dEnergy values. Overall correlation values are presented in black, and linear fittings calculated for TCR-alpha and TCR-beta chains independently are presented in red and cyan respectively.*

Correlation between physicochemical properties of cognate CDR3 and epitope residues

Using “Peptides” and “HDMD” R packages, seven groups of amino acid descriptors were calculated for the contacting residues in CDR3 loops and peptides in original and mutated TCR-pMHC complex structures. It should be mentioned that only mutated positions were taken into account. The descriptor groups were as follows: Blosum indices (Blos1-Blos10), Kidera factors (*KF1-KF13*), VHSE (*VHSE1- VHSE 8*), Cruciani properties (*PP1-PP3*), zScales (*Z1-Z5*), FASGAI (*F1-F6*) and Atchley factors (PAH, PSS, MS, CC, EC) *(32)*.

The majority of calculated indices can be grouped according to the specific physicochemical features they represent: hydrophobicity, steric properties, electronic, and secondary structure features (**Table 3**).

The rest of the descriptors, for example, Blosum4 - Blosum9 correlate with several properties and the specific one cannot be prioritized.

To analyze the consistency between properties of contacting residues in CDR3 loops and epitopes, we performed rank correlation analysis of the corresponding factors and indices. Spearman correlations were calculated within selected groups of descriptors for all interacting residues, the closest contacting residues, and amino acid pairs interacting through at least one side chain group. The most valuable correlations in groups of descriptors were identified using the Shapiro-Wilk test. Paired correlations and their distribution for selected groups of indices are presented in **Figure 5**, and best correlations are listed in **Table 4**

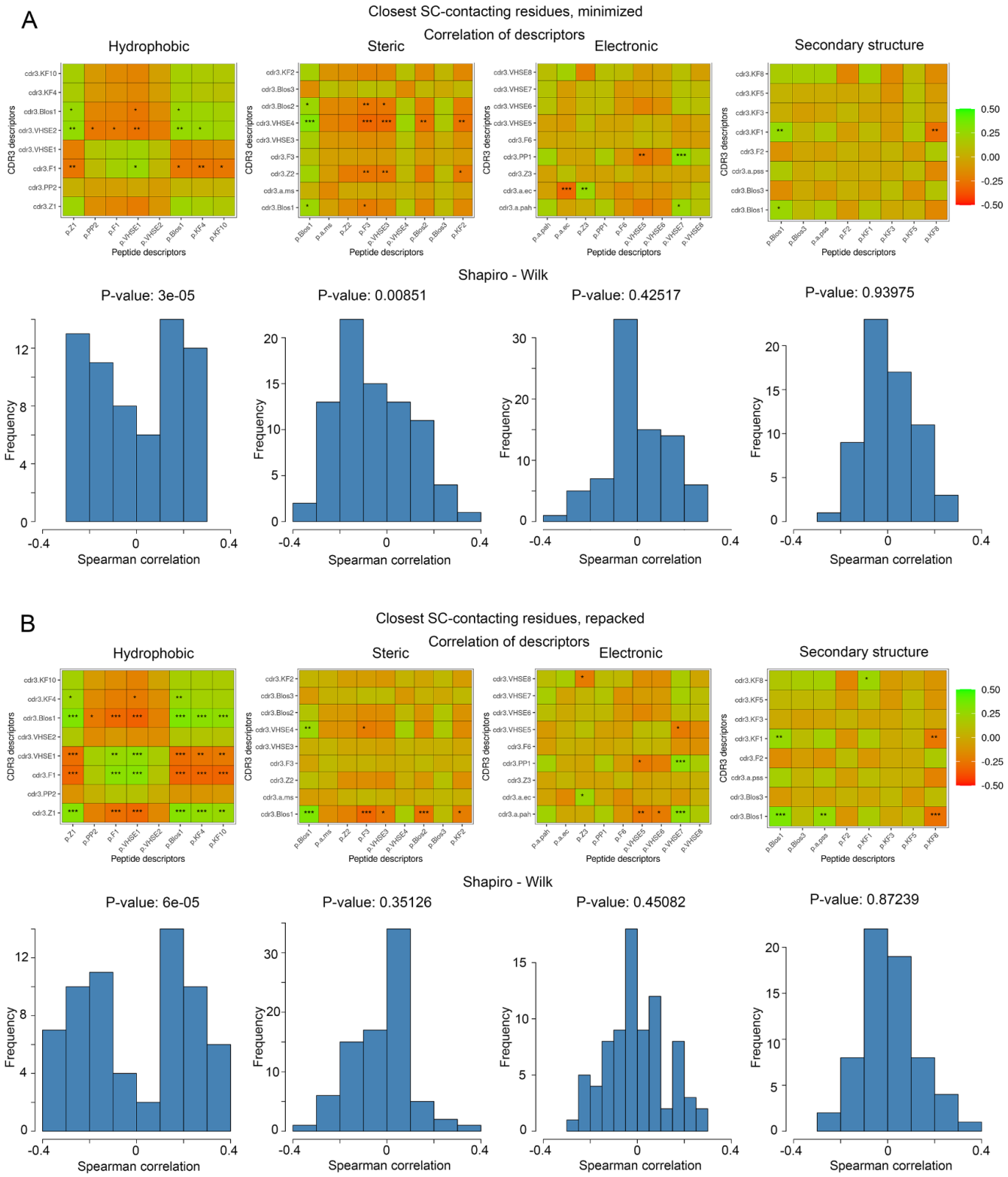

Figure 5. Correlations of calculated descriptors between contacting residues of CDR3 loops and epitopes.

The presented correlation analysis was performed for the closest contacting residues, interacting through at least one side-chain group in A) minimized and B) repacked models. Paired correlation values are represented as waffle plots, and their distribution in groups is shown as histograms. Statistical significance of correlation is labeled with "", "**" and "***" for P-values < 0.05, 0.01 and 0.001 respectively.*

The best correlation values were calculated for the hydrophobic and steric groups of descriptors in minimized structures, and their distribution was non-normal, according to the Shapiro–Wilk test (p-values were $3x10^{-5}$ and 0.0085, respectively). After repacking of modeled structures, which led to structural fitting of contacting residues and displacement of their side-chain groups, the correlations of steric descriptors became weaker, while the correlations of hydrophobic descriptors became more significant.

Identifying residue binding features in CDR3:peptide interface using machine learning

At the final stage we performed RFE (Recursive Feature Elimination) analysis and applied the random forest (RF) algorithm to make predictive models for the affinity values of contacting amino acid residue pairs in CDR3 loops and peptides. To include a wider range of valid pairwise contacts between CDR3 loops and TCRs, we calculated amino acid descriptors and energy values for known TCR-pMHC complexes available in the PDB database. In total, we added 152 structures of human T-cell receptors with peptides and MHC-I triple complexes to the analysis.

As our modeled structures were optimized using energy minimization or repacking of contacting residues, corresponding structures were treated separately and combined with selected resolved structures from the PDB database. The two extended datasets, containing 94 amino acid descriptors and affinity values (per-residue energies) were divided into training and testing sets in 70% to 30%proportion. Affinity values were converted to 5 groups (factors) using quantile values.

Discretizing the target variables is a common step in machine learning procedures such as Random Forest, and there are several reasons for doing so. First, dividing the affinity values into meaningful groups can make it easier to interpret the results. Second, discretizing the values can help mitigate the effects of outliers and noise in the data. Finally, it can be useful for classification tasks, such as predicting whether a given interaction is "strong" or "weak".

During RFE analysis of the extended datasets containing either minimized or repacked modeled structures, we identified 10 and 13 variables, respectively, as the most important predictors of the affinity values. These descriptors are presented in **Table 5**

Upon analyzing the selected descriptors, it is noticeable that most of them were calculated for amino acids from CDR3 loops, and the majority of the top 5 descriptors were related to the hydrophobic properties of the studied residues.

Evaluating the models built for the two selected datasets using testing data showed that the quality of their predictions was relatively similar for repacked and minimized structures.

The accuracy of the model built using minimized structures was 0.4212 with a 95% confidence interval of 0.3905 - 0.4524, and the accuracy of the second model was 0.448 with a 95% confidence interval of 0.417 - 0.4793. The Kappa statistic for the “minimized” model was 0.2765, and for the “repacked” model, it was 0.3098. The slightly higher accuracy of the model built using the extended data set of repacked structures and the higher Kappa statistic indicates better agreement between predicted and actual values compared to the second model built using minimized structures. The McNemar's Test P-Value was also lower for the “repacked” model, suggesting that it may be a more reliable model.

METHODS

Identification of CDR3 sequences clusters

Clustering of CDR3 sequences from the T-cell receptor sequences database VDJdb *(5)* was performed according to three main rules. First, a “core” of a cluster was designated by one of the CDR3 sequences presented in a PDB structure. Second, new CDR3 sequences (neighbors) were placed in the cluster if they could be generated step-by-step introducing single amino acid substitutions one at a time. The CDR3 sequences should have the same lengths, so no deletions or insertions were allowed. Additionally, the V- and J- genes of corresponding TCRs should be the same as the one carrying the “core” CDR3 loop. Pairing of TCRα - TCRβ chains was not taken into account. Third, the Hamming distance between the core and each of the neighbor CDR3 sequences in the cluster was limited to 3. Thus, the mutation path from the CDR3 sequence from the PDB database and the most diverse sequence in the cluster should consist of not more than 3 consequent single mutations. The validation of our proposed modeling approach and the explanation of why we selected a limit of 3 mutations is discussed in **Supplementary Note 1**.

Step-by-step modeling of CDR3 loops

A Rosetta package *(33)* was used to implement an *in silico* single amino acid mutation modeling approach. The Rosettascripts mover “MutateResidue” was used to replace selected residues while retaining main chain heavy atom positions according to the initial template structures, modifying only side chain atoms.

Further structural and energy optimization was performed using the relax protocol with additional restraints on atom coordinates, L-BFGS minimization algorithm and ref2015 score function. Additionally, the repacking protocol of Rosettascripts was used to optimize contacting residues in modeled TCR – peptide - MHC complexes. Repacking was performed for CDR3 loop and peptide residues situated closer than 5Å from each other, as these residues were estimated as contacting in modeled complexes.

Structural data analysis

Identification of close CDR3 and peptide residues in modeled complexes was performed using in house Java and Bash scripts. Contacting parts of residues (side and main chains) were identified using RING *(34)* software.

Calculation of energy values of contacting TCR-pMHC interfaces in modeled structures, as well as *RMSD* values between modeled and original CDR3 loop structures was performed using Rosetta score_jd2 application. Energy values were calculated using three variations of Rosetta ref2015 scoring function: “full” ref2015 energy function with all default energy terms included, and two “limited” variations, set by lists of selected terms. The first preset (“Large patch”) included *fa_atr* (attractive portion of the Lennard Jones potential), *fa_sol* (Lazaridis-Karplus solvation energy), *hbond_sr_bb* (h-bond energy, short-range backbone-backbone), *hbond_lr_bb* (bond energy, long-range backbone-backbone), *hbond_bb_sc* (h-bond energy, backbone-sidechain) and *hbond_sc* (h-bond energy, sidechain-sidechain) energy terms. The second (“Small patch”) consisted of the same terms as the “Large patch”, except for *hbond_sr_bb* and *hbond_bb_sc*.

Amino acid descriptors and indices were calculated using “Peptides” (Blosum indices, Kidera factors, VHSE, Cruciani properties, zScales, FASGAI) and “HDMD” (Atchley factors) packages in R *(35,36)*.

Statistical analysis and machine learning

Statistical analysis of computed energy values of the modeled structures and properties of contacting amino acid residues in TCR-pMHC complexes was performed using R packages. RFE analysis was performed on the training set consisting of 94 amino acid descriptors, calculated for contacting amino acid residues in CDR3 loops of TCRs and peptides to select the most important descriptors for predicting the target variable. Random forest algorithm was then used to train a model, which was used to make predictions on the testing set. Per-residue energy values were grouped into 5 clusters and used as target variables during the RFE analysis and RF modeling. The performance of the model was evaluated using confusion matrix analysis. Calculations and data preparation were performed using Caret and RandomForest packages in R.

Discussion

In this study we proposed an *in silico* approach for template-based modeling of highly homological CDR3 loops in full TCR - peptide – MHC complexes using stepwise introduction of single amino acid substitutions.

Using our approach, we modeled 1517 structures based on 29 templates.Upon analyzing these structures, we showed that widely used standard Blosum62 and Blosum100 scores do not correlate with possible impacts of amino acid mutations in CDR3 loops on binding energy during TCR – epitope recognition as long as those substitutions appear in non-contacting parts of loops. This finding suggests that the analysis and comparison of CDR3 sequences in context of epitope recognition should mainly consider contacting residues and not be limited to simple sequence alignments.

Also, we found that contacting residues in CDR3b can have a greater effect on TCR–peptide recognition than those in CDR3a loops. This conclusion is based on the analysis of the impact

of CDR3 amino acid variations on interaction energy values, depending on their remoteness from peptides and correlation between Blosum indices and calculated absolute values of dEnergy of interacting interfaces. In both cases corresponding properties and values of CDR3b residues showed better correlations in comparison to CDR3a.

Analysis of physicochemical properties of contacting residues in CDR3 loops and epitopes, described by different descriptors, showed that hydrophobicity may be the main factor governing recognition and affinity of binding between CDR3 loops and epitopes in TCR-pMHC complexes.

In all statistical analyses in this study correlation values were moderate: -0.4 for distance - dEnergy and -0.22 for Blosum - dEnergy relations. Absolute correlation values calculated during the descriptor analysis did not exceed 0.33. That may indicate that all studied variations of amino acid residues may not have a significant impact on binding of CDR3 loops to peptides in order to preserve T-cell receptor's ability.

Acknowledgements

This work was supported by grant № 075-15-2019-1789 from the Ministry of Science and Higher Education of the Russian Federation.

Table 1. Details for initial PDB templates and the number VDJdb entries modeled as structures.

Dash ("-") indicates there were no VDJdb records with 1-3 mismatches we could model using our approach.

Template annotation							Modeled structures	
PDB	**Peptide**	**TCRα V-gene**	**TCRα J-gene**	**TCRβ V-gene**	**TCRβ J-gene**	**MHC gene**	**Unique CDR3α**	**Unique CDR3β**
5nqk	ELAGIGILTV	TRAV12-2*01	TRAJ45*01	TRBV19*01	TRBJ2-2*01	HLA-A2	1	-
5nht	ELAGIGILTV	TRAV12-2*01	TRAJ45*01	TRBV19*01	TRBJ2-2*01	HLA-A2	4	-
2nx5	EPLPQGQLTAY	TRAV1-2*01	TRAJ6*01	TRBV10-3*01	TRBJ1-5*01	HLA-B35	5	4
1mi5	FLRGRAYGL	TRAV26-2*01	TRAJ52*01	TRBV7-8*01	TRBJ2-7*01	HLA-B8	-	5
5isz	GILGFVFTL	TRAV24*01	TRAJ27*01	TRBV19*01	TRBJ2-7*01	HLA-A2	-	2
5euo	GILGFVFTL	TRAV27*01	TRAJ37*01	TRBV19*01	TRBJ2-7*01	HLA-A2	61	216
2vlr	GILGFVFTL	TRAV27*01	TRAJ42*01	TRBV19*01	TRBJ2-7*01	HLA-A2	29	79
1oga	GILGFVFTL	TRAV27*01	TRAJ42*01	TRBV19*01	TRBJ2-7*01	HLA-A2		
2vlj	GILGFVFTL	TRAV27*01	TRAJ42*01	TRBV19*01	TRBJ2-7*01	HLA-A2		
2vlk	GILGFVFTL	TRAV27*01	TRAJ42*01	TRBV19*01	TRBJ2-7*01	HLA-A2		
5e6i	GILGFVFTL	TRAV35*01	TRAJ37*01	TRBV27*01	TRBJ2-2*01	HLA-A2	5	2
5jhd	GILGFVFTL	TRAV38-2 /DV8*01	TRAJ52*01	TRBV19*01	TRBJ1-2*01	HLA-A2	1	83
3o4l	GLCTLVAML	TRAV5*01	TRAJ31*01	TRBV20-1*01	TRBJ1-2*01	HLA-A2	17	23
3mv7	HPVGEADYFEY	TRAV20*01	TRAJ58*01	TRBV9*01	TRBJ2-2*01	HLA-B35	7	6

3mv8	HPVGEADYFEY	TRAV20*01	TRAJ58*01	TRBV9*01	TRBJ2-2*01	HLA-B35		
3mv9	HPVGEADYFEY	TRAV20*01	TRAJ58*01	TRBV9*01	TRBJ2-2*01	HLA-B35		
4pri	HPVGEADYFEY	TRAV20*01	TRAJ58*01	TRBV9*01	TRBJ2-2*01	HLA-B35		
2ypl	KAFSPEVIPMF	TRAV5*01	TRAJ13*01	TRBV19*01	TRBJ1-2*01	HLA-B57	3	18
4g9f	KRWIIMGLNK	TRAV14DV4*01	TRAJ21*01	TRBV6-5*01	TRBJ1-1*01	HLA-B27	-	2
1ao7	LLFGYPVYV	TRAV12-2*01	TRAJ24*01	TRBV6-5*01	TRBJ2-7*01	HLA-A2	1	-
4ftv	LLFGYPVYV	TRAV12-2*01	TRAJ24*01	TRBV6-5*01	TRBJ2-7*01	HLA-A2		
3gsn	NLVPMVATV	TRAV24*01	TRAJ49*01	TRBV6-5*01	TRBJ1-2*01	HLA-A2	3	-
5d2l	NLVPMVATV	TRAV24*01	TRAJ49*01	TRBV7-2*01	TRBJ2-5*01	HLA-A2	8	20
5d2n	NLVPMVATV	TRAV26-2*01	TRAJ43*01	TRBV7-6*01	TRBJ1-4*01	HLA-A2	17	19
6vmx	RPPIFIRRL	TRAV24*01	TRAJ37*01	TRBV4-1*01	TRBJ1-2*01	HLA-B7	2	-
4mji	TAFTIPSI	TRAV17*01	TRAJ22*01	TRBV7-3*01	TRBJ2-2*01	HLA-B51	1	1
7n6e	YLQPRTFLL	TRAV12-1*01	TRAJ43*01	TRBV19*01	TRBJ2-2*01	HLA-A2	68	-
7n1f	YLQPRTFLL	TRAV12-2*01	TRAJ30*01	TRBV7-9*01	TRBJ2-7*01	HLA-A2	15	34
7rtr	YLQPRTFLL	TRAV12-2*01	TRAJ30*01	TRBV7-9*01	TRBJ2-7*01	HLA-A2		

Table 2. Correlation values, calculated for Blosum scores and absolute values of dEnergy after the introduction of amino acid substitutions in modeled complexes.

	All mutations		Contacting mutations			
Blosum index	**Pearson correlation**	**P-value**	**Pearson correlation**	**P-value**	**Energy scoring**	**Optimization**
BLA.62.v2	-0.136	**2.03E-04**	-0.219	**7.76E-06**	Small patch	Minimized
BLA.62.v2	-0.135	**2.36E-04**	-0.205	**2.69E-05**	Large patch	Minimized
SIJ.62.v2	-0.112	**0.002**	-0.182	**2.16E-04**	Small patch	Minimized
SIJ.100.v2	-0.097	**0.008**	-0.165	**6.67E-11**	Small patch	Minimized
SIJ.62.v2	-0.107	**0.004**	-0.164	**0.001**	Large patch	Minimized
BLA.100.v2	-0.096	**0.009**	-0.164	**1.86E-10**	Small patch	Minimized
BLA.62.v2	-0.135	**4.34E-05**	-0.161	**3.07E-04**	Large patch	Repacked
SIJ.100.v2	-0.084	**0.022**	-0.137	**0.005**	Large patch	Minimized
BLA.100.v2	-0.083	**0.024**	-0.136	**0.006**	Large patch	Minimized
BLA.62.v2	-0.123	**1.79E-04**	-0.133	**0.003**	Small patch	Repacked
BLA.62.v2	-0.055	0.119	-0.128	**0.008**	Rosetta	Minimized
SIJ.62.v2	-0.117	**4.01E-04**	-0.126	**0.005**	Large patch	Repacked
SIJ.62.v2	-0.050	0.154	-0.113	**0.019**	Rosetta	Minimized
SIJ.100.v2	-0.107	**0.001**	-0.110	**0.014**	Large patch	Repacked
SIJ.62.v2	-0.082	**0.011**	-0.109	**0.015**	Rosetta	Repacked
SIJ.100.v2	-0.085	**0.009**	-0.102	**0.023**	Rosetta	Repacked
BLA.100.v2	-0.106	**0.001**	-0.099	**0.026**	Large patch	Repacked
BLA.100.v2	-0.038	0.287	-0.099	**0.040**	Rosetta	Minimized
BLA.62.v2	-0.071	**0.028**	-0.097	**0.029**	Rosetta	Repacked
SIJ.100.v2	-0.040	0.261	-0.097	**0.044**	Rosetta	Minimized

Table 3 Groups of studied amino acid descriptors

Names of the Atchley indices were shortened using "a." prefix

Property	**Amino acid indices**
Hydrophobicity	Z1, PP2, F1, VHSE1, VHSE2, Blos1, KF4, KF10
Steric properties	a.ms, Z2, F3, VHSE3, VHSE4, Blos1, Blos2, Blos3, KF2
Electronic properties	a.pah, a.ec, Z3, PP1, F6, VHSE5, VHSE6, VHSE7, VHSE8
Secondary structure	a.pss, F2, Blos1, Blos3, KF1, KF3, KF5, KF8

Table4 Top correlation values between calculated CDR3 and epitope residues indices.

A. Positive correlations

Descriptor type	CDR3 descriptor	Peptide descriptor	Correlation	p-value	p-value (adjusted)	Optimization and contact type
Steric	VHSE4	p.Blos1	**0.32**	1.09E-09	4.15E-06	Minimized, closest, side-chain
Hydrophobic	Blos1	Z1	**0.33**	4.93E-11	1.86E-07	Repacked, closest, side-chain
	Z1	Blos1	**0.31**	6.34E-10	2.40E-06	
	F1	VHSE1	**0.31**	9.46E-10	3.57E-06	
	Blos1	KF4	**0.30**	3.88E-09	1.46E-05	

B. Negative correlations

Descriptor type	CDR3 descriptor	Peptide descriptor	Correlation	p-value	p-value (adjusted)	Optimization and contact type
Steric	VHSE6	VHSE5	**-0.30**	1.13E-08	4.27E-05	Minimized, closest, side-chain
	VHSE6	F5	**-0.31**	4.09E-09	1.54E-05	
	Blos1	F3	**-0.31**	8.2E-10	3.09E-06	Repacked, closest, side-chain
Hydrophobic	Blos3	F3	**-0.30**	2.95E-09	1.11E-05	Repacked, closest, side-chain
	Z1	VHSE1	**-0.31**	1.96E-09	7.41E-06	
	F1	Z1	**-0.31**	6.1E-10	2.30E-06	
	F1	KF4	**-0.32**	5.59E-10	2.11E-06	
	F1	Blos1	**-0.32**	3.22E-10	1.21E-06	
	F1	KF10	**-0.32**	2.82E-10	1,07E-06	
	Blos1	VHSE1	**-0.33**	8.12E-11	3.07E-07	
Electronic	a.ec	a.ec	**-0.31**	6.59E-09	2.49E-05	Minimized, closest, side-chain

Table 5. Selected amino acid descriptors during Random Feature Elimination procedure.

The cells are colored according to the physico chemical properties of corresponding descriptors using the following color scheme: cyan – hydrophobic, orange – electronic, gray – steric, yellow -secondary structure. The top-5 descriptors according to the calculated importance are highlighted in bold font.

The properties represented by the descriptors are labeled as follows: H- hydrophobic, E - electronic, S- steric, SS - secondary structure

Minimized + original	**Repacked + original**
p.F1 (H)	**p.F1 (H)**
cdr3.VHSE1 (H)	**cdr3.VHSE1 (H)**
cdr3.Z1 (H)	**cdr3.Z1 (H)**
cdr3.KF10 (H)	**cdr3.KF10 (H)**
cdr3.KF4 (H)	cdr3.KF4 (H)
cdr3.VHSE7 (E)	cdr3.VHSE7 (E)
cdr3.Blos8	cdr3.VHSE8 (E)
cdr3.a.ms (S)	cdr3.a.ms (S)
p.a.cc	cdr3.F2 (SS)
cdr3.KF7	**cdr3.KF7**
	cdr3.Blos7
	cdr3.F5
	cdr3.Blos10

References

1. La Gruta NL, Gras S, Daley SR, Thomas PG, Rossjohn J. Understanding the drivers of MHC restriction of T cell receptors. Nat Rev Immunol. 2018 Jul;18(7):467–78.
2. Schatz DG, Swanson PC. V(D)J recombination: mechanisms of initiation. Annu Rev Genet. 2011 Aug;45:167–202.
3. Goldrath AW, Bevan MJ. Selecting and maintaining a diverse T-cell repertoire. Nature. 1999 Nov;402(6759):255–62.
4. Lee CH, Salio M, Napolitani G, Ogg G, Simmons A, Koohy H. Predicting Cross-Reactivity and Antigen Specificity of T Cell Receptors. Front Immunol. 2020 Oct;11:565096.
5. Goncharov M, Bagaev D, Shcherbinin D, Zvyagin I, Bolotin D, Thomas PG, et al. VDJdb in the pandemic era: a compendium of T cell receptors specific for SARS-CoV-2. Nat Methods. 2022 Sep;19(9):1017–9.
6. Vita R, Mahajan S, Overton JA, Dhanda SK, Martini S, Cantrell JR, et al. The Immune Epitope Database (IEDB): 2018 update. Nucleic Acids Res. 2019 Jan;47(D1):D339–43.
7. Tickotsky N, Sagiv T, Prilusky J, Shifrut E, Friedman N. McPAS-TCR: a manually curated catalogue of pathology-associated T cell receptor sequences. Bioinformatics. 2017 Sep;33(18):2924–9.
8. Gowthaman R, Pierce BG. TCR3d: The T cell receptor structural repertoire database. Bioinformatics. 2019 Dec;35(24):5323–5.
9. Berman HM, Westbrook J, Feng Z, Gilliland G, Bhat TN, Weissig H, et al. The Protein Data Bank. Nucleic Acids Res. 2000 Jan;28(1):235–42.
10. Gowthaman R, Pierce BG. TCRmodel: high resolution modeling of T cell receptors from sequence. Nucleic Acids Res. 2018 Jul;46(W1):W396–401.
11. Jensen KK, Rantos V, Jappe EC, Olsen TH, Jespersen MC, Jurtz V, et al. TCRpMHCmodels: Structural modelling of TCR-pMHC class I complexes. Sci Rep. 2019 Oct;9(1):14530.
12. Bradley P. Structure-based prediction of T cell receptor:peptide-MHC interactions. Elife. 2023 Jan;12.
13. Schritt D, Li S, Rozewicki J, Katoh K, Yamashita K, Volkmuth W, et al. Repertoire Builder: high-throughput structural modeling of B and T cell receptors. Mol Syst Eng. 2019 Aug;4(4):761–8.
14. Klausen MS, Anderson MV, Jespersen MC, Nielsen M, Marcatili P. LYRA, a webserver for lymphocyte receptor structural modeling. Nucleic Acids Res. 2015 Jul;43(W1):W349-55.
15. Reynisson B, Alvarez B, Paul S, Peters B, Nielsen M. NetMHCpan-4.1 and NetMHCIIpan-4.0: improved predictions of MHC antigen presentation by concurrent motif deconvolution and integration of MS MHC eluted ligand data. Nucleic Acids Res. 2020 Jul;48(W1):W449–54.
16. Li S, Wilamowski J, Teraguchi S, van Eerden FJ, Rozewicki J, Davila A, et al. Structural Modeling of Lymphocyte Receptors and Their Antigens. Methods Mol Biol. 2019;2048:207–29.
17. Grazioli F, Mösch A, Machart P, Li K, Alqassem I, O'Donnell TJ, et al. On TCR binding predictors failing to generalize to unseen peptides. Front Immunol. 2022 Oct;13:1014256.
18. Dhusia K, Su Z, Wu Y. A structural-based machine learning method to classify binding affinities between TCR and peptide-MHC complexes. Mol Immunol. 2021 Nov;139:76–86.
19. Crean RM, Pudney CR, Cole DK, van der Kamp MW. Reliable In Silico Ranking of Engineered Therapeutic TCR Binding Affinities with MMPB/GBSA. J Chem Inf Model. 2022 Feb;62(3):577–90.
20. Peacock T, Chain B. Information-Driven Docking for TCR-pMHC Complex Prediction.

Front Immunol. 2021 Jun;12:686127.
21. Zhu Y, Huang C, Su M, Ge Z, Gao L, Shi Y, et al. Characterization of amino acid residues of T-cell receptors interacting with HLA-A*02-restricted antigen peptides. Ann Transl Med. 2021 Mar;9(6):495.
22. Wu D, Efimov GA, Bogolyubova AV, Pierce BG, Mariuzza RA. Structural insights into protection against a SARS-CoV-2 spike variant by T cell receptor (TCR) diversity. J Biol Chem. 2023 Feb;103035.
23. Szeto C, Nguyen AT, Lobos CA, Chatzileontiadou DSM, Jayasinghe D, Grant EJ, et al. Molecular Basis of a Dominant SARS-CoV-2 Spike-Derived Epitope Presented by HLA-A*02:01 Recognised by a Public TCR. Cells. 2021 Oct;10(10).
24. Chaurasia P, Nguyen THO, Rowntree LC, Juno JA, Wheatley AK, Kent SJ, et al. Structural basis of biased T cell receptor recognition of an immunodominant HLA-A2 epitope of the SARS-CoV-2 spike protein. J Biol Chem. 2021 Sep;297(3):101065.
25. Wu D, Kolesnikov A, Yin R, Guest JD, Gowthaman R, Shmelev A, et al. Structural assessment of HLA-A2-restricted SARS-CoV-2 spike epitopes recognized by public and private T-cell receptors. Nat Commun. 2022 Jan;13(1):19.
26. Davis MM, Bjorkman PJ. T-cell antigen receptor genes and T-cell recognition. Nature. 1988 Aug;334(6181):395–402.
27. Krogsgaard M, Davis MM. How T cells “see” antigen. Nat Immunol. 2005 Mar;6(3):239–45.
28. Springer I, Besser H, Tickotsky-Moskovitz N, Dvorkin S, Louzoun Y. Prediction of Specific TCR-Peptide Binding From Large Dictionaries of TCR-Peptide Pairs. Front Immunol. 2020 Aug;11:1803.
29. Tynan FE, Reid HH, Kjer-Nielsen L, Miles JJ, Wilce MCJ, Kostenko L, et al. A T cell receptor flattens a bulged antigenic peptide presented by a major histocompatibility complex class I molecule. Nat Immunol. 2007 Mar;8(3):268–76.
30. Bagaev DV, Vroomans RMA, Samir J, Stervbo U, Rius C, Dolton G, et al. VDJdb in 2019: database extension, new analysis infrastructure and a T-cell receptor motif compendium. Nucleic Acids Res. 2020 Jan;48(D1):D1057–62.
31. Borrman T, Cimons J, Cosiano M, Purcaro M, Pierce BG, Baker BM, et al. ATLAS: A database linking binding affinities with structures for wild-type and mutant TCR-pMHC complexes. Proteins. 2017 May;85(5):908–16.
32. Atchley WR, Zhao J, Fernandes AD, Drüke T. Solving the protein sequence metric problem. Proc Natl Acad Sci U A. 2005 May;102(18):6395–400.
33. Leaver-Fay A, Tyka M, Lewis SM, Lange OF, Thompson J, Jacak R, et al. ROSETTA3: an object-oriented software suite for the simulation and design of macromolecules. Methods Enzym. 2011;487:545–74.
34. Martin AJM, Vidotto M, Boscariol F, Di Domenico T, Walsh I, Tosatto SCE. RING: networking interacting residues, evolutionary information and energetics in protein structures. Bioinformatics. 2011 Jul;27(14):2003–5.
35. Osorio D, Rondón-Villarreal P, Torres R. Peptides: A package for data mining of antimicrobial peptides. R J. 2015;7(1):4.
36. R Core Team. R: A language and environment for statistical computing. R Foundation for Statistical Computing.
37. Lindahl, Abraham, Hess, Spoel V der. GROMACS 2020 Manual. 2020.
38. McLachlan AD. Rapid comparison of protein structures. Acta Crystallogr A. 1982 Jan;38(6):871–3.

Supplementary Information

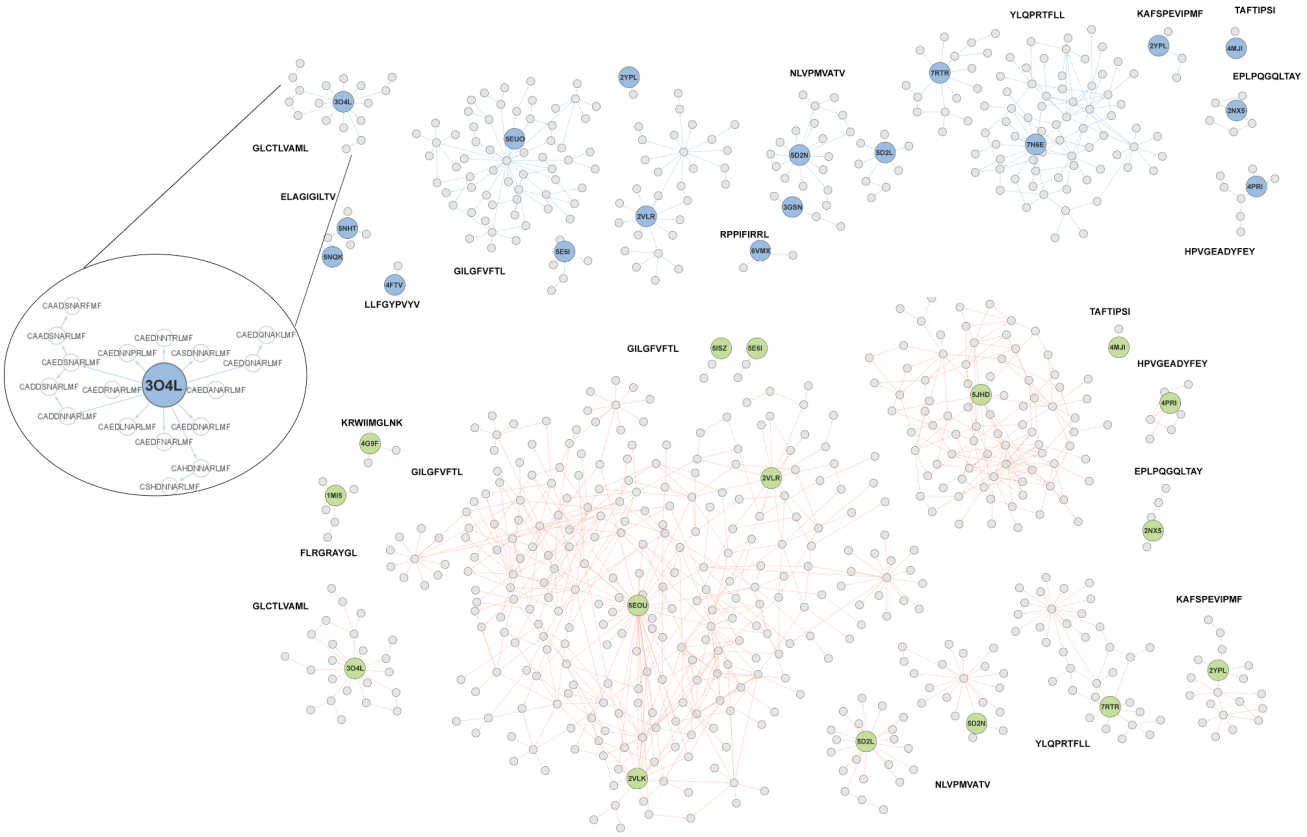

Figure S1 Graph with paths used for stepwise modeling of CDR3 loops. *CDR3α sequences are connected with blue edges and sequences of CDR3β – red. Initial templates are presented as circles with PDB identifiers and are colored blue in CDR3α and green in CDR3β clusters. Epitope labels are placed near corresponding connected components.*

CDR3α	CDR3β	Peptide	PDBs
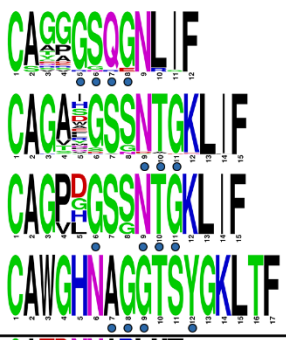		GILGFVFTL	2vlj 2vlk 2vlr 1oga 5euo 5e6i 5jhd
		GLCTLVAML	3o4l
		HPVGEADYFEY	3mv7 3mv8 3mv9 4pri
		KAFSPEVIPMF	2ypl
		KRWIIMGLNK	4g9f
	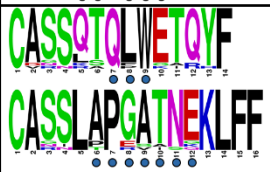	NLVPMVATV	5d2l 5d2n 3gsn
		RPPIFIRRL	6vmx
		TAFTIPSI	4mji
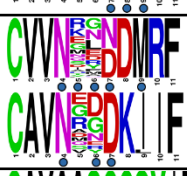		YLQPRTFLL	7n6e 7n1f 7rtr
		EPLPQGQLTAY	2nx5
		FLRGRAYGL	1mi5
		ELAGIGILTV	5nht

Figure S2. Logo-formatted sequences of CDR3 loops in modeled structures. *Residues, contacting with peptides are marked with blue circles.*

Table S1. Number of paired CDR3 – epitope contacting residues in modeled structures.

"All contacts"- all contacting pairs formed by mutated residue of CDR3 loops with epitope amino acids, situated closer than 5Å apart.

"SC- contacting"- contacting pairs formed by mutated residue of CDR3 loops with epitope amino acids, situated closer than 5Å apart. At least one residue in the pair interacts by its side chain group.

"Closest contacts" – only the closest residue of epitope selected for each mutated residue of CDR3 loop in each modeled structure.

"Closest SC-contacts" - only the closest, interacting by at least one side chain group, residues of epitope selected for each mutated residue of CDR3 loop in each modeled structure.

	All contacts		**SC-contacts**		**Closest contacts**		**Closest SC-contacts**	
Minimized	**1022**		**584**		**537**		**346**	
	CDR3a	CDR3b	CDR3a	CDR3b	CDR3a	CDR3b	CDR3a	CDR3b
	302	720	203	381	176	361	114	232
Repacked	**1060**		**635**		**569**		**370**	
	CDR3a	CDR3b	CDR3a	CDR3b	CDR3a	CDR3b	CDR3a	CDR3b
	323	737	195	440	176	393	101	269

Supplementary Note 1

Validation of the proposed stepwise single amino acid substituting modeling approach

Materials and methods

TCR-pMHC homology modeling.

Modeling of the selected TCR structures was performed using our approach, TCR-pMHC modeling *(11)* service and TCRModel algorithm *(10)* implemented in the Rosetta package. The models were selected based on their sequence similarity to known templates from the PDB database. CDR3 loops were modeled by introducing less than 6 amino acid substitutions starting from the known template, and the resulting "target" TCR chain should also be resolved in the PDB database. During modeling using TCRModel, target structures were eliminated from the templates library. TCR-pMHC modeling was performed using the online service with default settings (http://www.cbs.dtu.dk/services/TCRpMHCmodels/index.php). These models were used to validate our modeling and optimization approaches.

In addition to energy minimization and repacking of close-contacting residues, loop refinement was performed for our models using a kinematic protocol implemented in the LoopRemodel Rosettascripts mover. During the refinement procedure the four terminal residues (two residues at the N-terminus and two - at C-terminus) of the CDR3 loop were fixed, while the rest of the backbone and side chains were allowed to be flexible.

Molecular dynamics

Molecular dynamics simulations were carried out using Gromacs-2020.5 software package *(37)*. The systems were neutralized by adding Na^+ and Cl^- , and solvated with TIP3P water models. MD calculations were performed using the Amber99-SB force field. Energy minimization was sequentially performed in vacuum and in solvation for 150,000 steps. Subsequently, temperature was increased to 300K and pressure was set to 1 atm using NVT and NPT ensembles, respectively. Molecular dynamics simulations were performed on 50 ns trajectories with 2 fs time steps.

Results

Minimization vs. repacking of TCR-pMHC contacting area.

Initial visual inspection of some previously modeled complexes using our approach revealed sterical issues that can occur during spatial positioning of large amino acid residues instead of small ones, and their orientation was altered depending on the final optimization step. For

example, finalizing repacking optimization led to the misplacement of Arg and Tyr side chain groups in mutated β-chain CDR3 loop from 2VLR PDB structure (**Figure SN1**) compared to a structure received after energy minimization only. To validate the stability of these modeled structures, we performed molecular dynamics calculations for three selected pMHC-TCR complexes: two modeled structures with the “CASSIRWAYEQYF” CDR3 loop of the beta-chain of TCR, built based on 2VLR PDB structures with just energy minimization or repacking of contacting residues as the final optimization step; and the original 2VLR PDB structure that was used as an initial template for the modeling process.

During the analysis of the MD trajectories, the most attention was paid to the displacement of peptide-MHC complex with respect to TCR since the observed displacement of side chain groups in contacting residues might influence the stability of the TCR-pMHC interaction. It was shown that in the original TCR-pMHC complex structure (PDB id: 2VLR) the pMHC position was the most stable (**Fig.SN1D**). RMSD values for the peptide-MHC molecules were in the range of 3.5-5A during molecular dynamics.

On the other hand, the modeled complex that was built using only energy minimization as the final optimization step was unstable (**Figure SN1D**), and the MHC molecule with the peptide dramatically shifted from their initial position during MD (**Figure SN1B**). Such low affinity of this modeled complex might be explained by a bad structural “complementary” in the TCR-pMHC contacting interface due to the unfavorable positioning of replaced side chain groups.

Changes in RMSD values for the MHC-peptide molecules in the third (repacked) complex showed that at the beginning of molecular dynamics, the pMHC complex shifted from its initial pose and returned back after 15 - 20 ns of MD.The alteration of MHC-TCR docking pose is shown in **Figure SN1C**.

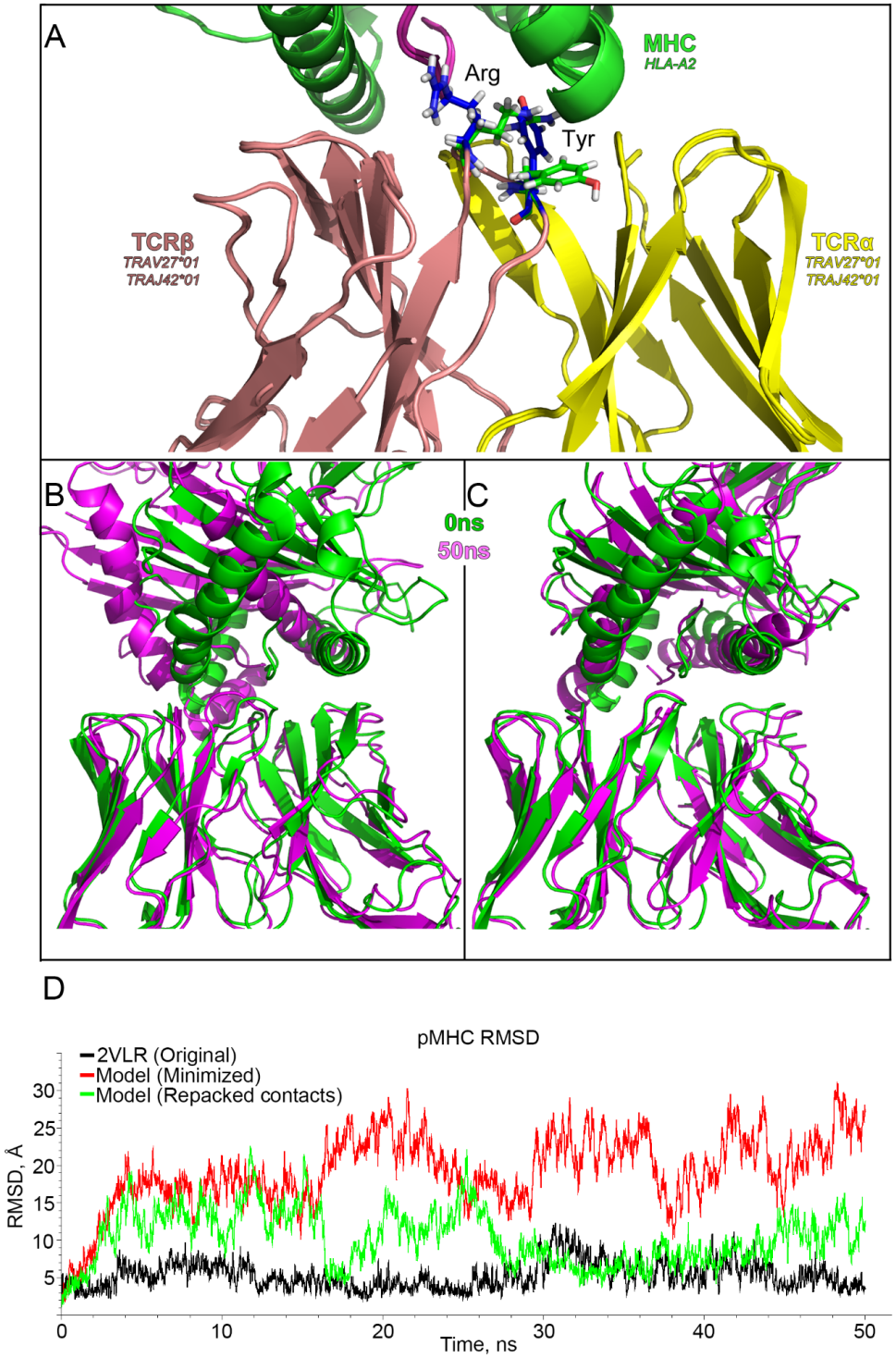

Figure SN1 *Stability of the original and modeled TCR-pMHC complexes and structural comparison of CDR3 loops after energy minimization or repacking of contacting residues.*

A) Spatial displacement of Arg and Tyr side chain groups after repacking of contacting residues in pMHC – TCR complex built from 2VLR. *Repacked amino acids are colored blue, mutated and just minimized structures are green.*

B) Displacement of the peptide-MHC complex during molecular dynamics of just minimized modeled structures and C) after repacking of the contacting interface.

D) RMSD values, calculated for peptide-MHC complexes during molecular dynamics. Values of the original PDB structure (2VLR) are represented as a green line, minimized modeled structure - as black, and repacked modeled structure - as red. All structures of complexes were aligned by TCR chains.

These results show that repacking of contacting residues might be a necessary step while modeling CDR3 loops in TCR-pMHC complexes using our step-by-step single mutation approach to achieve more stable complexes and cover larger conformational space of TCR-pMHC contacting interfaces.

Validation of modeling approaches using reference PDB structures.

To validate the proposed mutation modeling approach and compare our results with corresponding models built using available TCR modeling services, we analyzed sequences of all CDR3 loops of ternary TCR-pMHC complexes available in the PDB database. All found sequences were pairwise aligned separately for TCR-alpha and TCR-beta chains. Analyzing the built alignments, we selected 27 CDR3 sequences that could be modeled by introducing up to 6 sequential substitutions starting from some other template structures presented in the PDB database. Hereinafter, the number of introduced amino acid substitutions will be referred to as the “mutation order”. The list of all selected CDR3 sequences with initial templates for the modeling process and their original PDB structures is presented in **Table SN1**

Table SN1 *Structures, used for validation of modeling approaches*

PDB template	TCR	CDR3	PDB original	Order
3qeq	TRA	CAFITGNQFYF	5d2l	2
5e6i	TRA	CAGAIGPSNTGKLIF	5euo	3
3qdm	TRA	CARNTGNQFYF	3gsn	2
1ao7	TRB	CASRPGLMSAQPEQYF	4ftv	4

5yxn	TRB	CASRRGSAELYF	5yxu	3
2vlr	TRB	CASSDTVSYEQYF	5nme, 5nmf, 5nmg	3
5nmg	TRB	CASSDWVSYEQYF	1lp9, 2j8u, 2jcc, 2uwe	1
6bj2	TRB	CASSFNMATGQYF	5brz, 5bs0	5
1oga	TRB	CASSIRSSYEQYF	5euo, 5hho	1
2vlj	TRB	CASSIRSSYEQYF	5euo, 5hho	1
5euo	TRB	CASSIRSSYEQYF	5hho	1
4l3e	TRB	CASSLSFGTEAFF	3qdg, 3qdj, 6am5, 6amu	1
5wkf	TRB	CASSPVTGGIYGYTF	3gsn	5
6avf	TRB	CASSQTQLWETQYF	5d2l	4
2vlj	TRB	CASSSRASYEQYF	2vlr	1
2vlr	TRB	CASSSRSSYEQYF	1oga, 2vlj, 2vlk, 2xn9, 4c56, 5hhm	1
5euo	TRB	CASSSRSSYEQYF	1oga, 2vlj, 2vlk, 2xn9, 4c56, 5hhm	1
4mji	TRB	CASSSWDTGELFF	3vxr, 3vxs	4
3qdg	TRB	CASSWSFGTEAFF	4l3e, 6d78, 6dkp	1
3vxr	TRB	CASSWSFGTEAFF	4l3e, 6d78, 6dkp	6

6amu	TRB	CASSWSFGTEAFF	4l3e, 6d78, 6dkp	1
2f53	TRB	CASSYLGNTGELFF	2p5e, 2p5w, 2pye	1
2p5w	TRB	CASSYVGNTGELFF	2bnq, 2bnr, 2f53, 2f54, 6q3s	1
4mnq	TRA	CAVDSATSGTYKYIF	4c56, 5men	4
5w1v	TRA	CAVLSSGGSNYKLTF	5eu6	4
5nqk	TRA	CAVSGGYQKVTF	2ypl	6
4g9f	TRA	CLVGEILDNFNKFYF	6avf	6

All T-cell receptor structures containing the selected CDR3 sequences were modeled using the TCRModel package of Rosetta software (10), TCR-pMHC modeling service (11) and our mutation approach. In addition to energy minimization and repacking of contacting residues, we performed a loop refinement procedure in our modeling approach as the final optimization step. Refinement was performed using Rosetta “LoopRemodel” mover with four “fixed” residues: two at each end of CDR3 loops.

As there can be some variability during conformational search and optimization of models, several runs of modeling were performed for each of the studied approaches: two runs of modeling were performed for our approach with different optimization procedures, two for the TCR-pMHC modeling service and three runs for TCRmodel.

RMSD values between compared structures were calculated using the Profit application (Martin, A.C.R. and Porter, C.T., http://www.bioinf.org.uk/software/profit/, (38)) separately for all atoms of CDR3 loops and for C-alpha atoms only. During the study all models were superposed with original (target) PDBs by corresponding TCR chains or by CDR3 loops. Thus, RMSD values, calculated for structures aligned by CDR3 loops, represent the “accuracy” of predictions of corresponding loop shapes, while alignment using TCR chains allows the evaluation of both the loop shapes and their orientation. Results are presented in **Figure SN2**.

If modeled structures constructed based on one template had several known original target structures, mean values were calculated for the corresponding deviations. RMSD values of different modeling runs are presented independently on the graph.

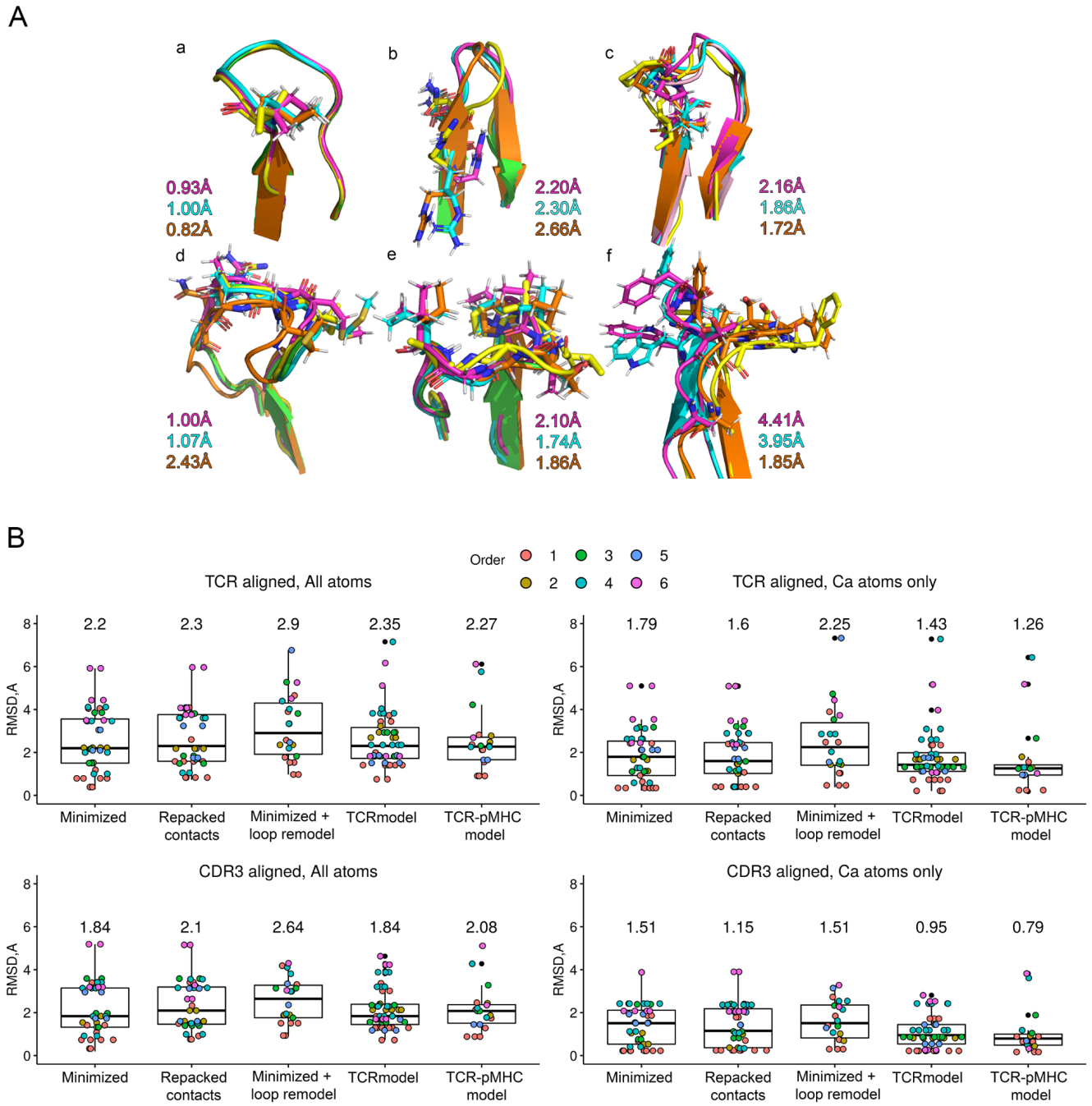

Figure SN2 *Comparison of modeled CDR3 structures with corresponding known conformations of CDR3 loops from PDB data bank.*

A) Structural comparison of models with different mutation orders. RMSD values, calculated for all atoms of CDR3 loops in structures aligned by TCR chains, are presented for three modeling approaches: our approach with energy minimization (magenta), our approach with

repacking of contacting residues (cyan) and TCRmodel (orange). Initial template structures are colored green and original structures with target CDR3 loops are colored yellow. CDR3 sequences and mutation orders are as follows: a) Mutation order = 1, CDR3 sequence: CASSIRSSYEQYF (TRB, original structure- 5hho, 5euo; template- 1oga), b) Mutation order = 2, CDR3 sequence: CARNTGNQFYF (TRA, original structure- 3gsn; template - 3qdm), c) Mutation order = 3, CDR3 sequence: CAGAIGPSNTGKLIF (TRA, original structure- 5euo; template - 5e6i), d) Mutation order = 4, CDR3 sequence: CASRPGLMSAQPEQYF (TRB, original structure- 4ftv; template - 1ao7), e) Mutation order = 5, CDR3 sequence: CASSPVTGGIYGYTF (TRB, original structure- 3gsn; template – 5wkf), f) Mutation order = 6, CDR3 sequence: CASSWSFGTEAFF (TRB, original structure- 4l3e; template - 3vxr)

B) Boxplots of RMSD values between modeled CDR3 conformations and loops from original PDB structures. Median values for each modeling approach are presented in corresponding boxes. Models built using the mutation approach with finalizing energy minimization are labeled as "Minimized + loop remodel" and "Minimized" depending on whether loop remodel algorithm was applied or not. Models refined by repacking of all contacting residues between pMHC and TCR are labeled "Repacked contacts", and models built using TCRModel or TCR-pMHC modeling approaches are labeled "TCRModel" and "TCR-pMHC model" respectively

Analysis of Cα atoms only in aligned CDR3 loops showed that all studied approaches allowed us to model conformations of the main chains of CDR3 loops close to the original structures. The median values for our approaches were 1.15Å for repacked structures and 1.51 Å for structures after just energy minimisation. The corresponding values for TCRmodel and TCR-pMHC modeling services were 0.95Å and 0.79Å.

Several outliers can be noted on the boxplots. These high RMSD values are associated with models carrying 6 substitutions (for all approaches) or 6-5 substitutions (for the TCR-pMHC model service).

As expected, median values of RMSD were higher during the analysis of full-atom structures of CDR3 loops including side-chain groups. The most significant increase was observed for structures modeled using the TCR-pMHC modeling service (from 0.79Å up to 2.08Å). The smallest median values were calculated for mutated structures with finalizing minimization and structures received using TCR-model (1.84Å for both mentioned approaches). CDR3 loops constructed using our approach with the loop refinement procedure at the final step had the lowest accuracy according to median RMSD values - 2.64Å during the analysis of structures aligned by CDR3 loops and 2.9Å for models aligned by corresponding TCR chains.

Analyzing all RMSD values, it can be observed that most of the modeled structures carrying from 4 up to 6 substitutions had lower accuracy than structures with mutation orders of 1-3. Median values of RMSD, calculated for structures carrying a different number of substitutions are presented in **Figure SN3**

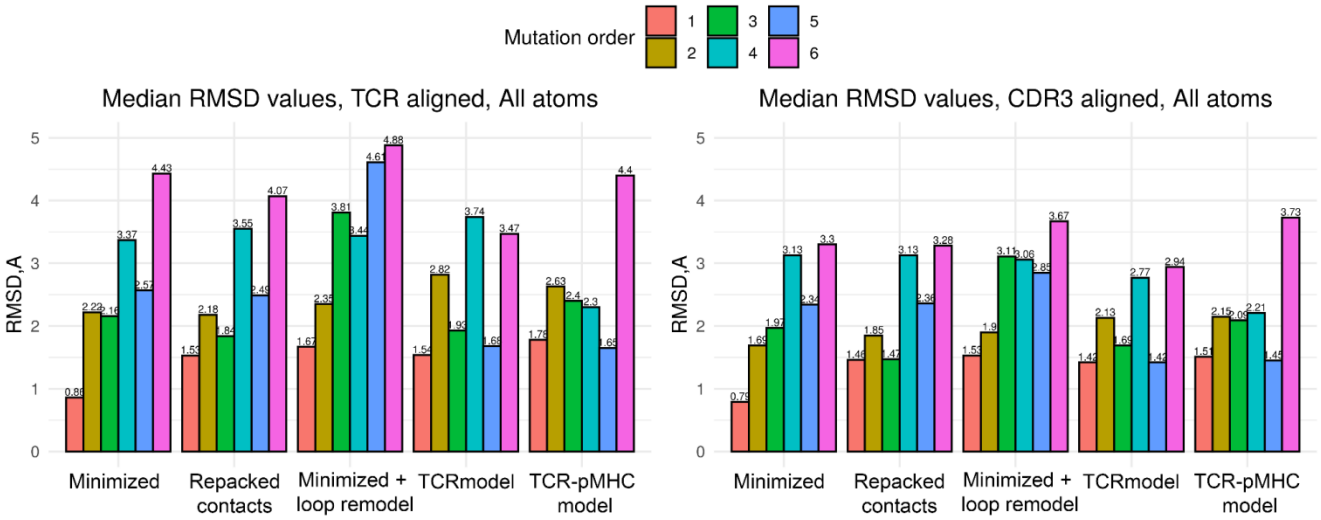

Figure SN3 *Median RMSD values, calculated for each mutation order individually*

It can be observed that the increase in RMSD values in all modeled structures correlated with the “mutation order”. According to the calculated RMSD values, the best models (closest to known structures) carried only one substitution and were built using our mutational protocol with only minimization as the final refinement step. The median values were 0.79Å and 0.86Å during the analysis of models aligned with the original structures by CDR3 loops and TCR chains, respectively. RMSD values for all other modeling approaches were in the range of 1.42Å -1.67 Å. The conformation and spatial orientation of CDR3 loops (**Fig. SN3**, TCR aligned, all atoms), carrying two substitutions, were better predicted by our approaches with median RMSD values between 2.18Å and 2.35Å. TCRmodel and TCR-pMHC modeling service predicted corresponding structures with 2.82Å and 2.63Å deviation, respectively. Third-order mutations were modeled with similar RMSD values among all tested approaches, and higher median deviation values were calculated for our approach with loop remodeling optimization.

According to median RMSD values starting from mutation order 4 and higher, the most accurate results were received using the TCR-pMHC modeling service. It could be explained by its modeling algorithm: the service uses its own templates database and there are no options to exclude target structures used in our benchmark. And, as far as we selected CDR3 loops that were available in the PDB database, TCR-pMHC models service could actually use them to perform homology modeling.

This validation step showed that our approach with finalizing energy minimization or repacking of contacting residues in TCR - pMHC interface can be used to model CDR3 loops carrying up to 3 mutations with an acceptable accuracy. However, loop refinement, on the other hand, can decrease the quality of models with 1-3 mutation order.

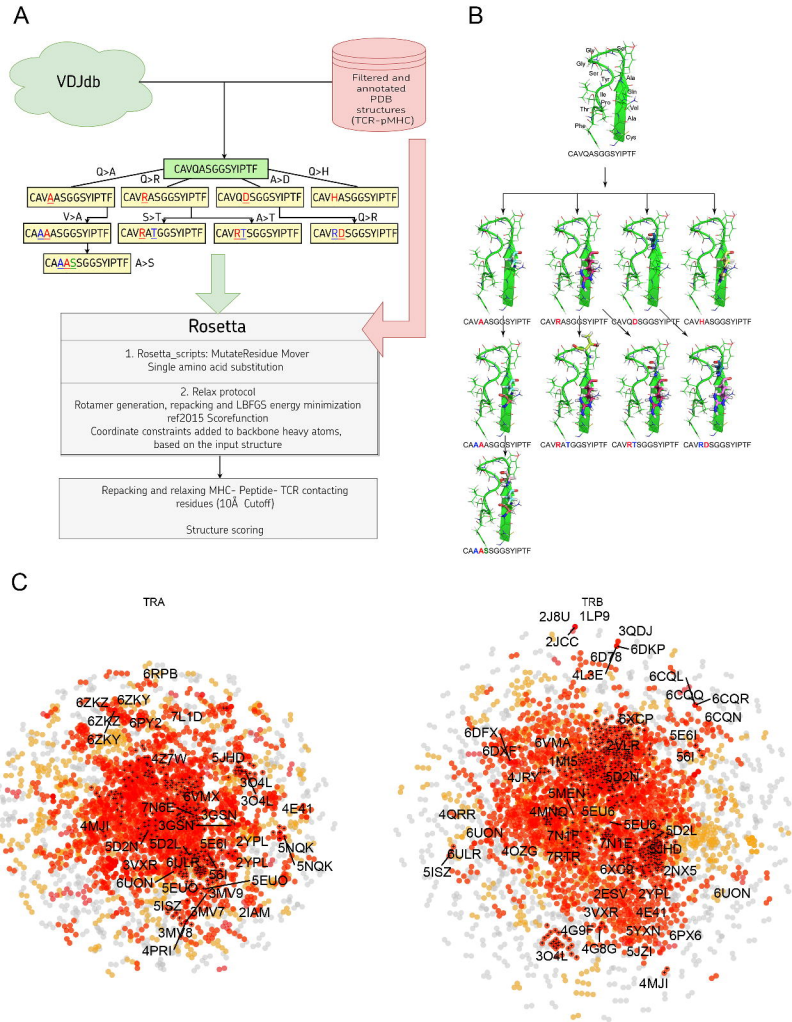
A
VDJdb
Filtered and annotated PDB structures (TCR-pMHC)
CAVQASGGSYIPTF
Q>A
Q>R
A>D
Q>H
CAVAASGGSYIPTF
CAVRASGGSYIPTF
CAVQDSGGSYIPTF
CAVHASGGSYIPTF
V>A
S>T
A>T
Q>R
CAAAASGGSYIPTF
CAVRATGGSYIPTF
CAVRTSGGSYIPTF
CAVRDSGGSYIPTF
CAAASSGGSYIPTF
A>S
Rosetta
1. Rosetta_scripts: MutateResidue Mover
Single amino acid substitution
2. Relax protocol
Rotamer generation, repacking and LBFGS energy minimization
ref2015 Scorefunction
Coordinate constraints added to backbone heavy atoms, based on the input structure
Repacking and relaxing MHC- Peptide- TCR contacting residues (10Å Cutoff)
Structure scoring
B
CAVQASGGSYIPTF
CAVAASGGSYIPTF
CAVRASGGSYIPTF
CAVQDSGGSYIPTF
CAVHASGGSYIPTF
CAAAASGGSYIPTF
CAVRATGGSYIPTF
CAVRTSGGSYIPTF
CAVRDSGGSYIPTF
CAAASSGGSYIPTF
C
TRA
6RPB
6ZKZ
6ZKY
6ZKZ
6PY2
7L1D
6ZKY
4Z7W
5JHD
3O4L
6VMX
3O4L
7N6E
3GSN
4E41
4MJI
3GSN
5D2N
5D2L
5E6I
2YPL
5NQK
3VXR
6ULR
2YPL
5NQK
6UON
5EUO
5EUO
3MV9
5ISZ
3MV7
2IAM
3MV8
4PRI
TRB
2J8U
1LP9
3QDJ
2JCC
6DKP
6D78
4L3E
6CQL
6CQQ
6CQR
6CQN
5XCP
6DFX
5E6I
6VMA
2VLR
6DXE
5I6I
1MI5
4JRY
5D2N
5MEN
4QRR
4MNQ
5EU6
5EU6
5D2L
6UON
7N1F
7N1E
5JHD
6ULR
4OZG
7RTR
6XC9
2NX5
5ISZ
2ESV
2YPL
6UON
3VXR
4E41
4G9F
5YXN
6PX6
3O4L
4G8G
5JZI
4MJI

Peptide - CDR3 contacts
All contacting residues
Peptide - CDR3 contacts
Closest contacting residues
Peptide - CDR3 contacts
SC-contacting residues
Peptide - CDR3 contacts
Closest SC-contacting residues
Peptide residue
CDR3 residue
K C H P E I M V R W A F Q G L S Y D N T
T N D Y S L G Q F A W R V M I E P H C K
Number of contacts
60
40
20
mut.n
20
40
60

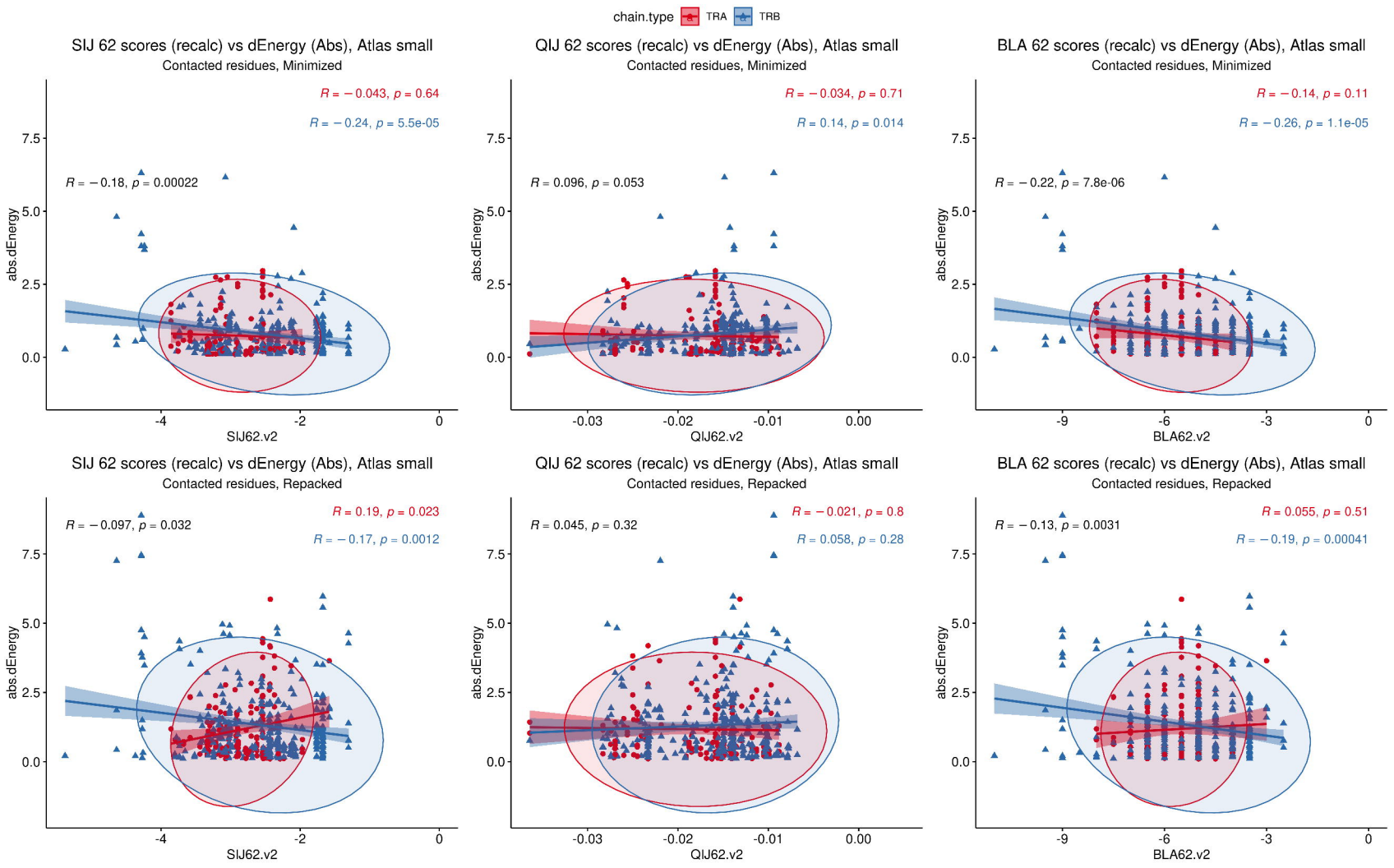
chain.type
TRA
TRB
SIJ 62 scores (recalc) vs dEnergy (Abs), Atlas small
Contacted residues, Minimized
R = −0.043, p = 0.64
R = −0.24, p = 5.5e-05
R = −0.18, p = 0.00022
abs.dEnergy
SIJ62.v2
QIJ 62 scores (recalc) vs dEnergy (Abs), Atlas small
Contacted residues, Minimized
R = −0.034, p = 0.71
R = 0.14, p = 0.014
R = 0.096, p = 0.053
QIJ62.v2
BLA 62 scores (recalc) vs dEnergy (Abs), Atlas small
Contacted residues, Minimized
R = −0.14, p = 0.11
R = −0.26, p = 1.1e-05
R = −0.22, p = 7.8e-06
BLA62.v2
SIJ 62 scores (recalc) vs dEnergy (Abs), Atlas small
Contacted residues, Repacked
R = 0.19, p = 0.023
R = −0.17, p = 0.0012
R = −0.097, p = 0.032
QIJ 62 scores (recalc) vs dEnergy (Abs), Atlas small
Contacted residues, Repacked
R = −0.021, p = 0.8
R = 0.058, p = 0.28
R = 0.045, p = 0.32
BLA 62 scores (recalc) vs dEnergy (Abs), Atlas small
Contacted residues, Repacked
R = 0.055, p = 0.51
R = −0.19, p = 0.00041
R = −0.13, p = 0.0031

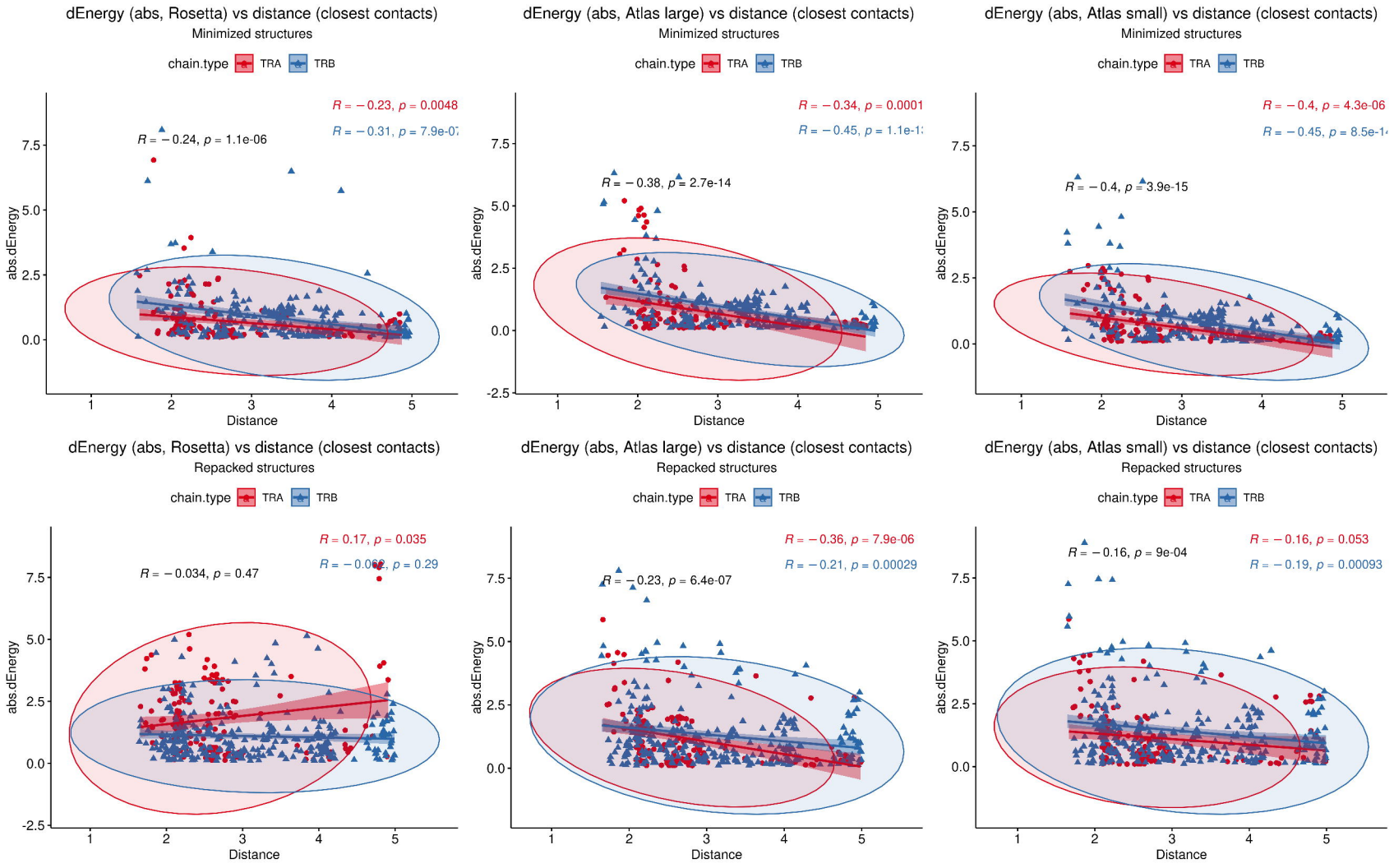
dEnergy (abs, Rosetta) vs distance (closest contacts)
Minimized structures
chain.type TRA TRB
R = −0.23, p = 0.0048
R = −0.31, p = 7.9e-07
R = −0.24, p = 1.1e-06
abs.dEnergy
Distance
dEnergy (abs, Atlas large) vs distance (closest contacts)
Minimized structures
chain.type TRA TRB
R = −0.34, p = 0.0001
R = −0.45, p = 1.1e-1
R = −0.38, p = 2.7e-14
abs.dEnergy
Distance
dEnergy (abs, Atlas small) vs distance (closest contacts)
Minimized structures
chain.type TRA TRB
R = −0.4, p = 4.3e-06
R = −0.45, p = 8.5e-1
R = −0.4, p = 3.9e-15
abs.dEnergy
Distance
dEnergy (abs, Rosetta) vs distance (closest contacts)
Repacked structures
chain.type TRA TRB
R = 0.17, p = 0.035
R = −0.062, p = 0.29
R = −0.034, p = 0.47
abs.dEnergy
Distance
dEnergy (abs, Atlas large) vs distance (closest contacts)
Repacked structures
chain.type TRA TRB
R = −0.36, p = 7.9e-06
R = −0.21, p = 0.00029
R = −0.23, p = 6.4e-07
abs.dEnergy
Distance
dEnergy (abs, Atlas small) vs distance (closest contacts)
Repacked structures
chain.type TRA TRB
R = −0.16, p = 0.053
R = −0.19, p = 0.00093
R = −0.16, p = 9e-04
abs.dEnergy
Distance

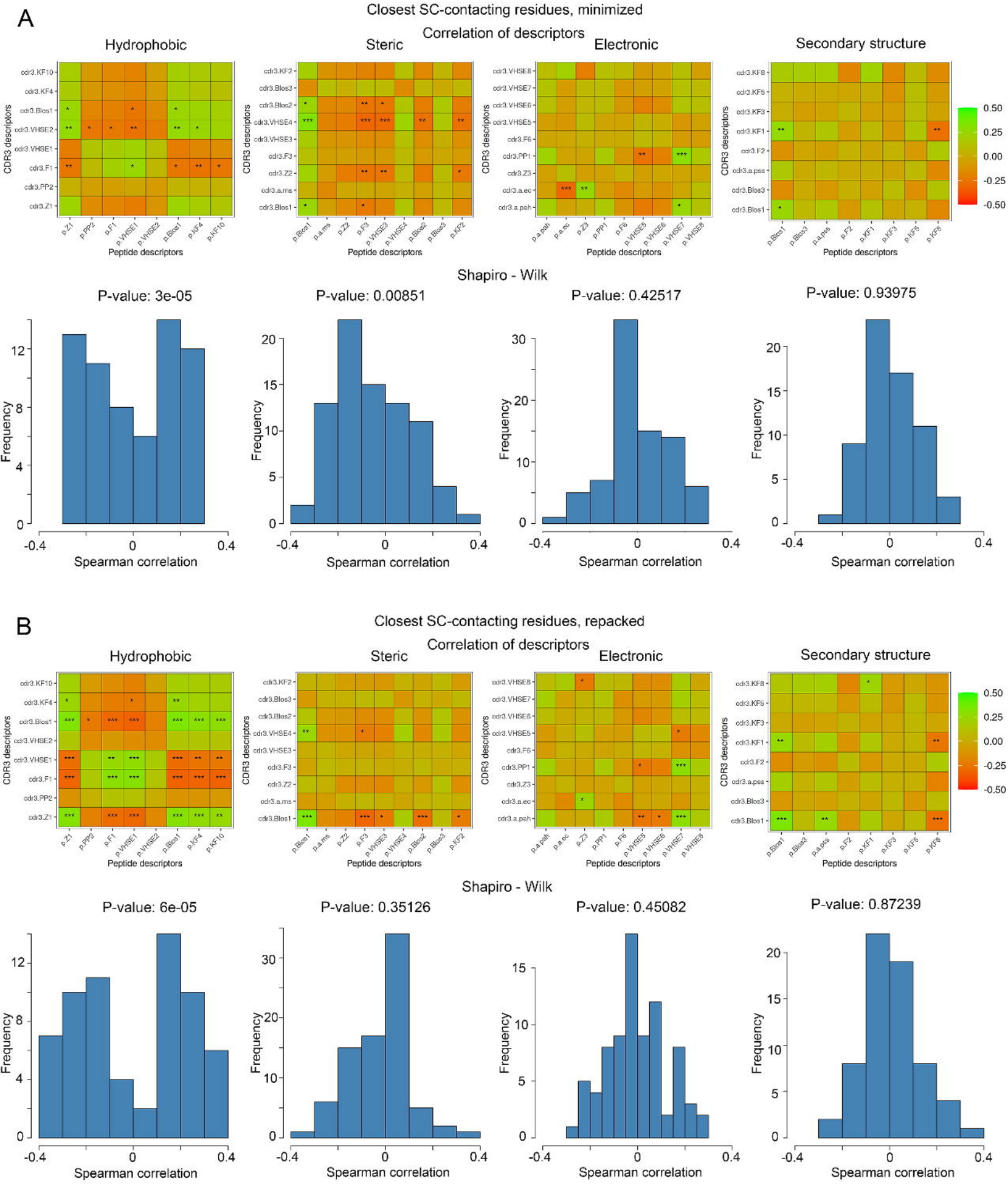
A
Closest SC-contacting residues, minimized
Correlation of descriptors
Hydrophobic
Steric
Electronic
Secondary structure
CDR3 descriptors
Peptide descriptors
Shapiro - Wilk
P-value: 3e-05
P-value: 0.00851
P-value: 0.42517
P-value: 0.93975
Frequency
Spearman correlation
B
Closest SC-contacting residues, repacked
Correlation of descriptors
Hydrophobic
Steric
Electronic
Secondary structure
CDR3 descriptors
Peptide descriptors
Shapiro - Wilk
P-value: 6e-05
P-value: 0.35126
P-value: 0.45082
P-value: 0.87239
Frequency
Spearman correlation

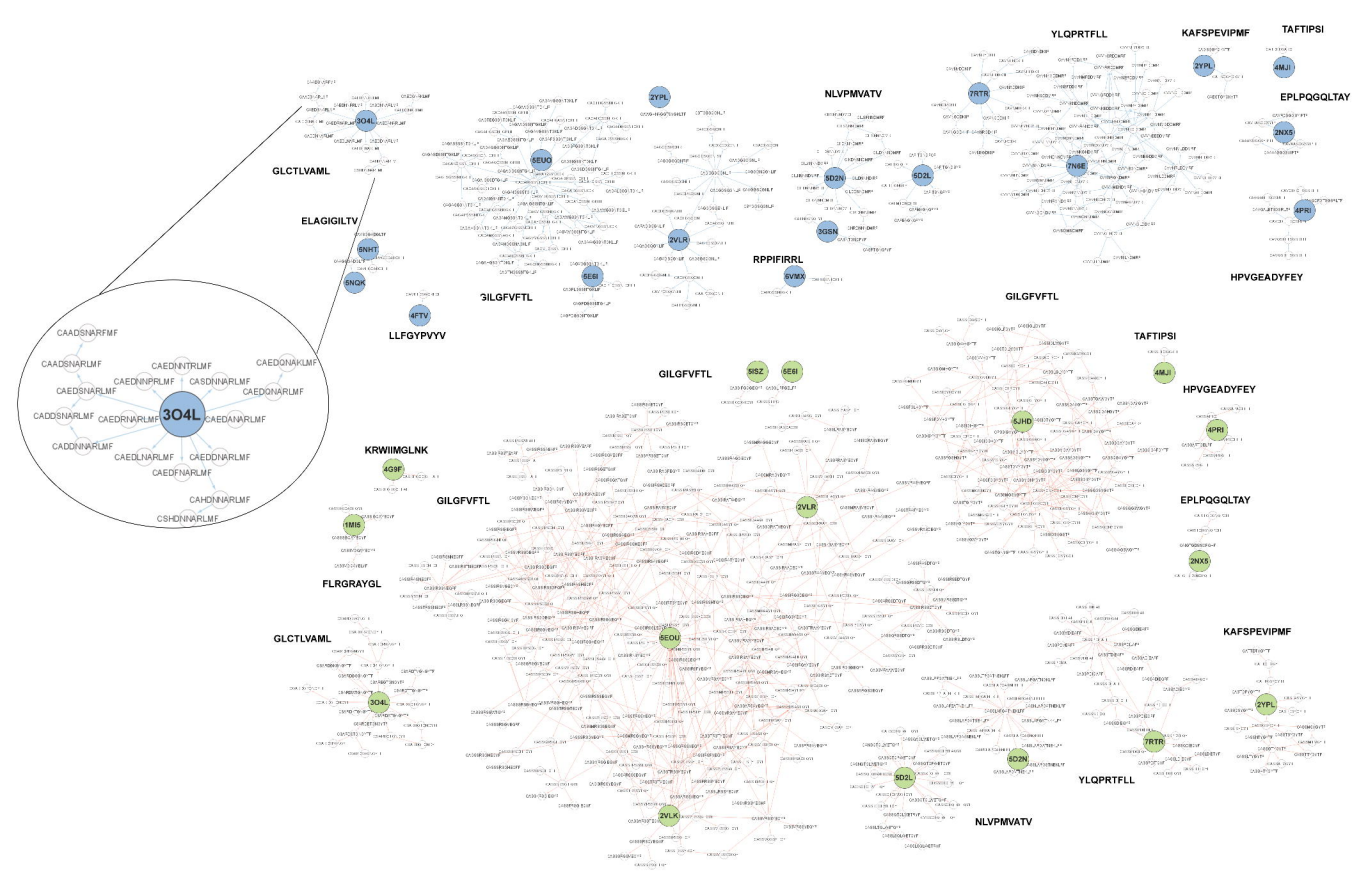

CAADSNARFMF
CAADSNARLMF
CAEDNNTRLMF
CAEDNAKLMF
CAEDNNPRLMF
CAEDNNARLMF
CAEDSNARLMF
CAEDNARLMF
CADDSNARLMF
CAEDRNARLMF
3O4L
CAEDANARLMF
CADDNNARLMF
CAEDLNARLMF
CAEDDNARLMF
CAEDFNARLMF
CAHDNNARLMF
CSHDNNARLMF
GLCTLVAML
ELAGIGILTV
LLFGYPVYV
KRWIIMGLNK
FLRGRAYGL
GLCTLVAML
GILGFVFTL
GILGFVFTL
GILGFVFTL
RPPIFIRRL
NLVPMVATV
NLVPMVATV
YLQPRTFLL
YLQPRTFLL
KAFSPEVIPMF
KAFSPEVIPMF
TAFTIPSI
TAFTIPSI
EPLPQGQLTAY
EPLPQGQLTAY
HPVGEADYFEY
HPVGEADYFEY
3O4L
3O4L
2YPL
5EUQ
2VLR
5EEI
5NHT
5NQK
4FTV
5SZ
5EEI
5SD2N
5SD2L
3GSN
5VMX
7RTR
7NSE
2YPL
4MJI
2NX5
4PRI
5JHD
4G9F
1MIS
2VLR
5EOU
2VLK
5SD2N
5SD2L
7RTR
2YPL
4MJI
4PRI
2NX5

CDR3α	CDR3β	Peptide	PDBs
	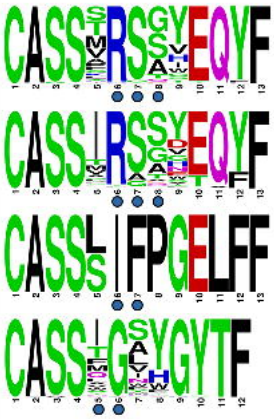	GILGFVFTL	2vlj 2vlk 2vlr 1oga 5euo 5e6i 5jhd
		GLCTLVAML	3o4l
		HPVGEADYFEY	3mv7 3mv8 3mv9 4pri
		KAFSPEVIPMF	2ypl
		KRWIIMGLNK	4g9f
   	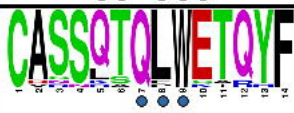 	NLVPMVATV	5d2l 5d2n 3gsn
		RPPIFIRRL	6vmx
		TAFTIPSI	4mji
 		YLQPRTFLL	7n6e 7n1f 7rtr
		EPLPQGQLTAY	2nx5
		FLRGRAYGL	1mi5
		ELAGIGILTV	5nht

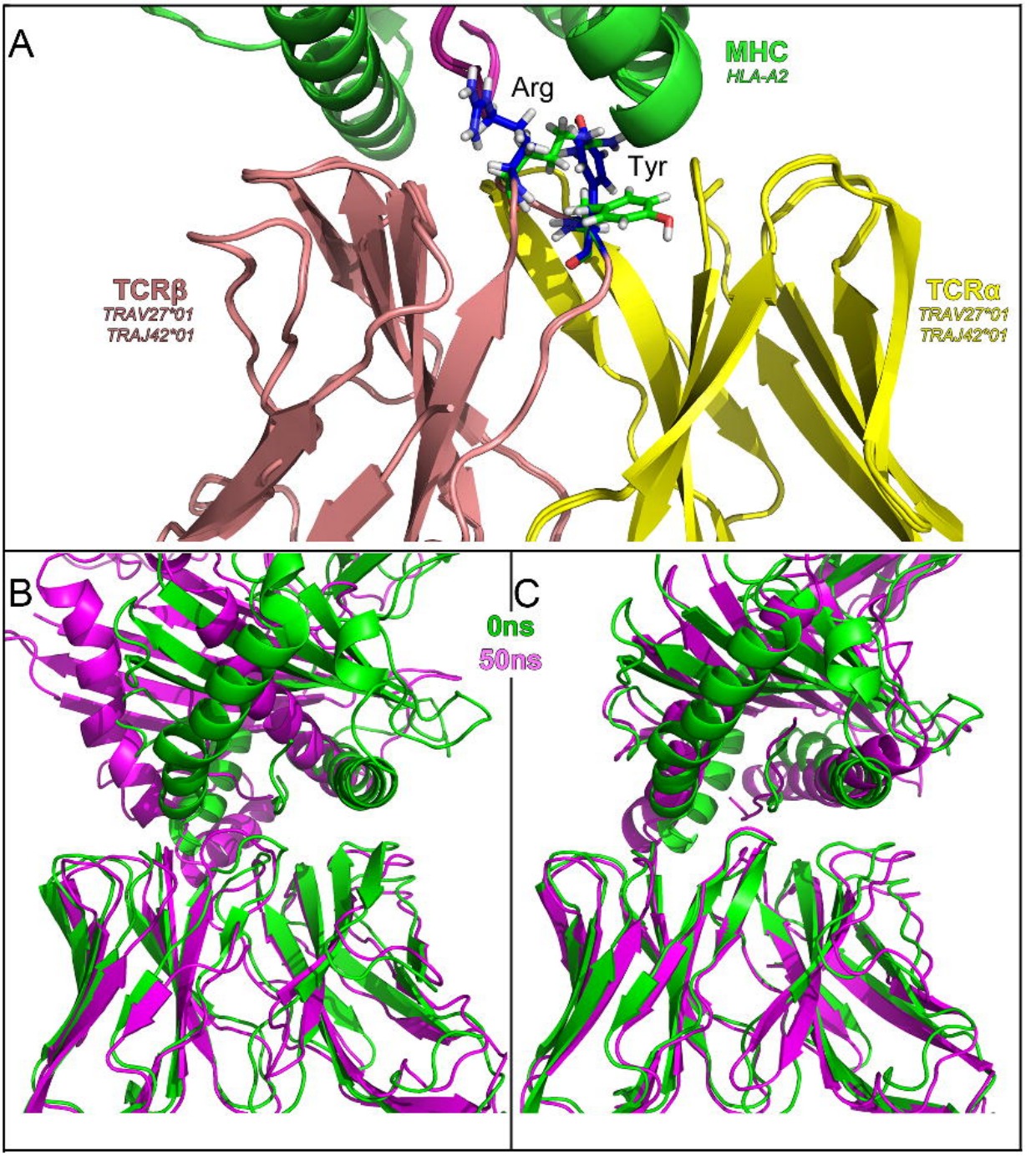
A
MHC
HLA-A2
Arg
Tyr
TCRβ
TRAV27*01
TRAJ42*01
TCRα
TRAV27*01
TRAJ42*01
B
C
0ns
50ns

D

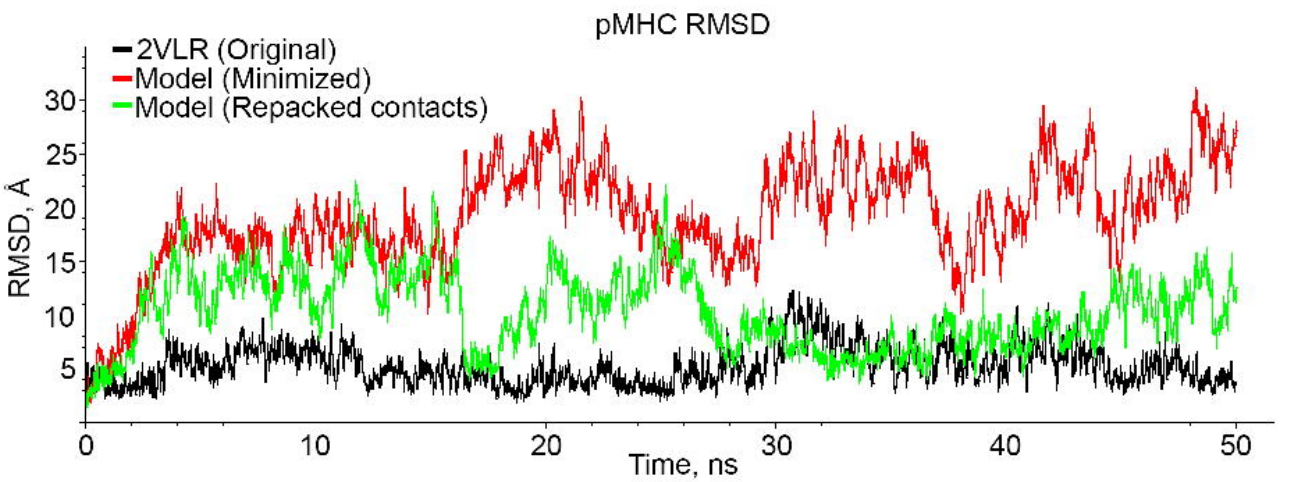
pMHC RMSD
2VLR (Original)
Model (Minimized)
Model (Repacked contacts)
RMSD, Å
Time, ns
0
10
20
30
40
50
5
10
15
20
25
30

A

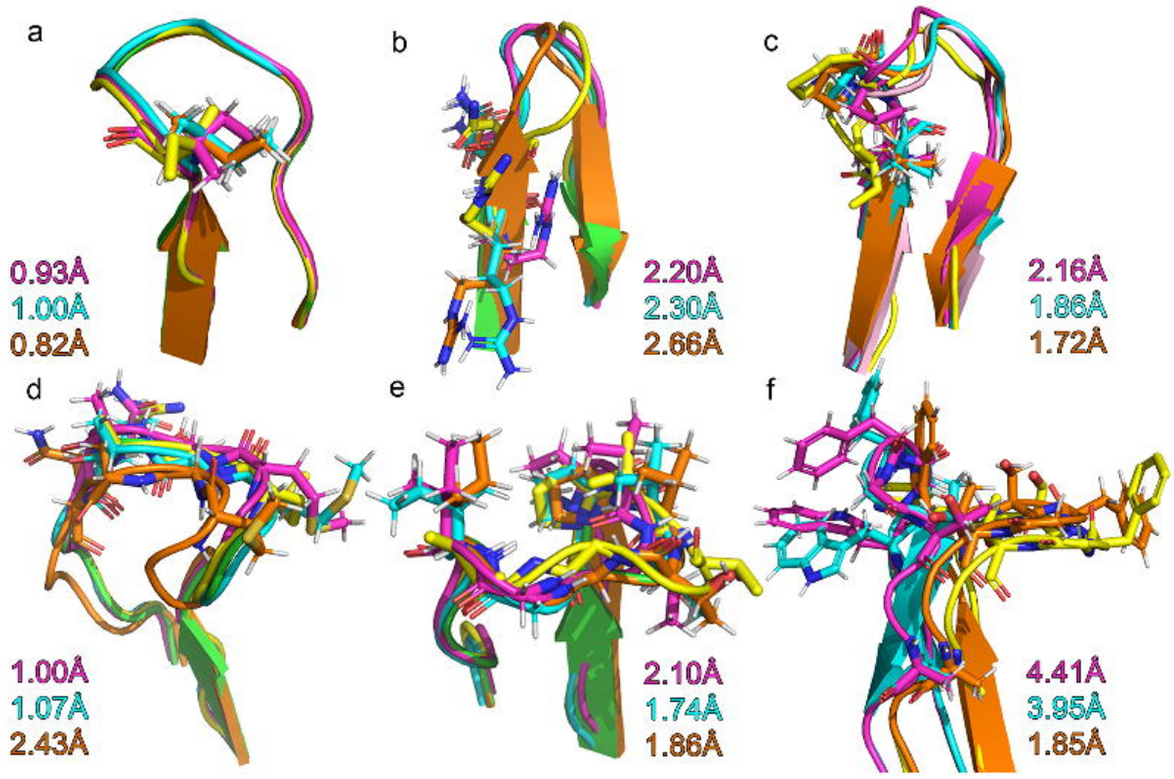
a
0.93Å
1.00Å
0.82Å
b
2.20Å
2.30Å
2.66Å
c
2.16Å
1.86Å
1.72Å
d
1.00Å
1.07Å
2.43Å
e
2.10Å
1.74Å
1.86Å
f
4.41Å
3.95Å
1.85Å

B

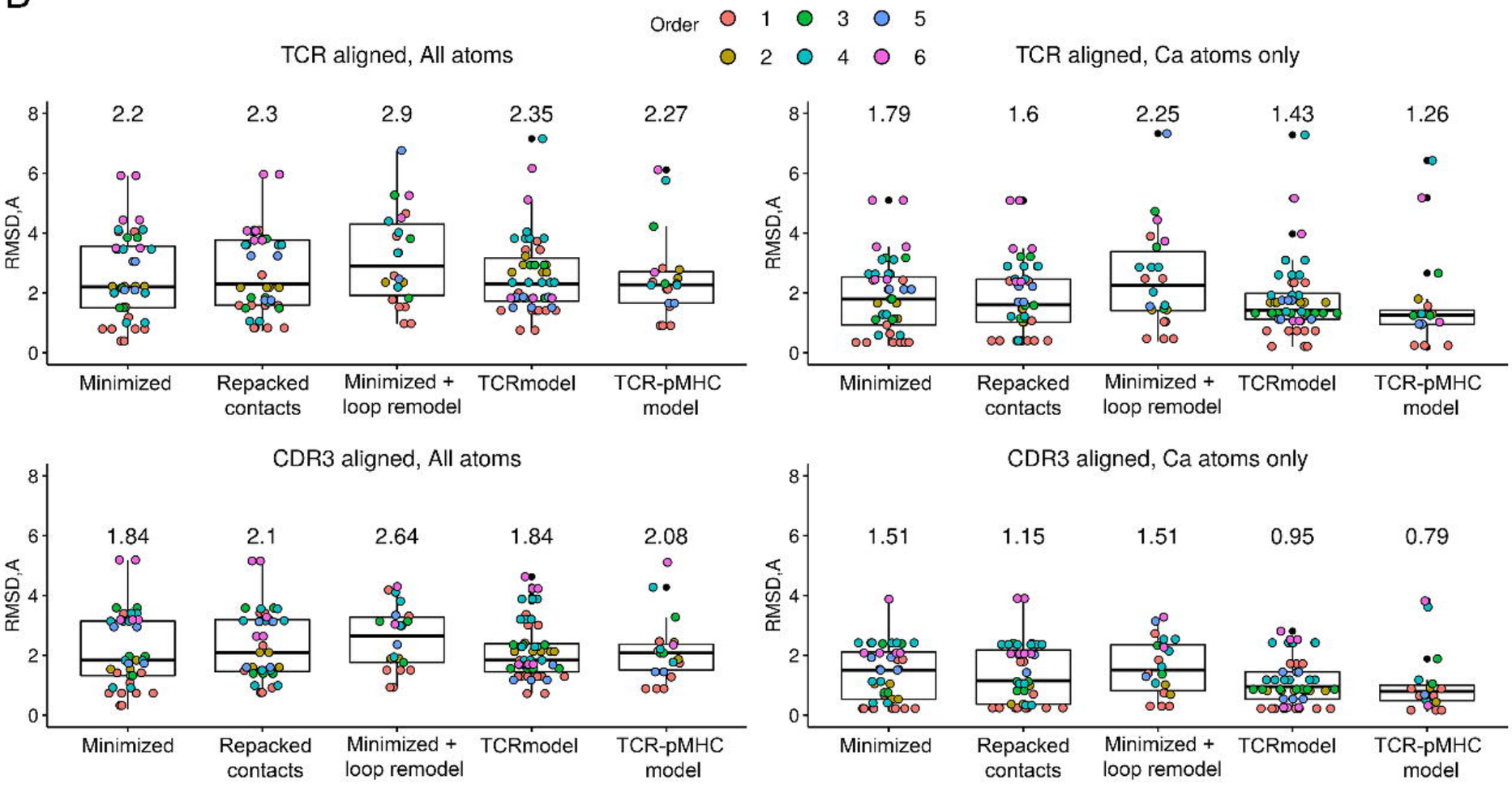
Order
1
2
3
4
5
6
TCR aligned, All atoms
2.2
2.3
2.9
2.35
2.27
TCR aligned, Ca atoms only
1.79
1.6
2.25
1.43
1.26
CDR3 aligned, All atoms
1.84
2.1
2.64
1.84
2.08
CDR3 aligned, Ca atoms only
1.51
1.15
1.51
0.95
0.79
RMSD,A
0
2
4
6
8
Minimized
Repacked contacts
Minimized + loop remodel
TCRmodel
TCR-pMHC model

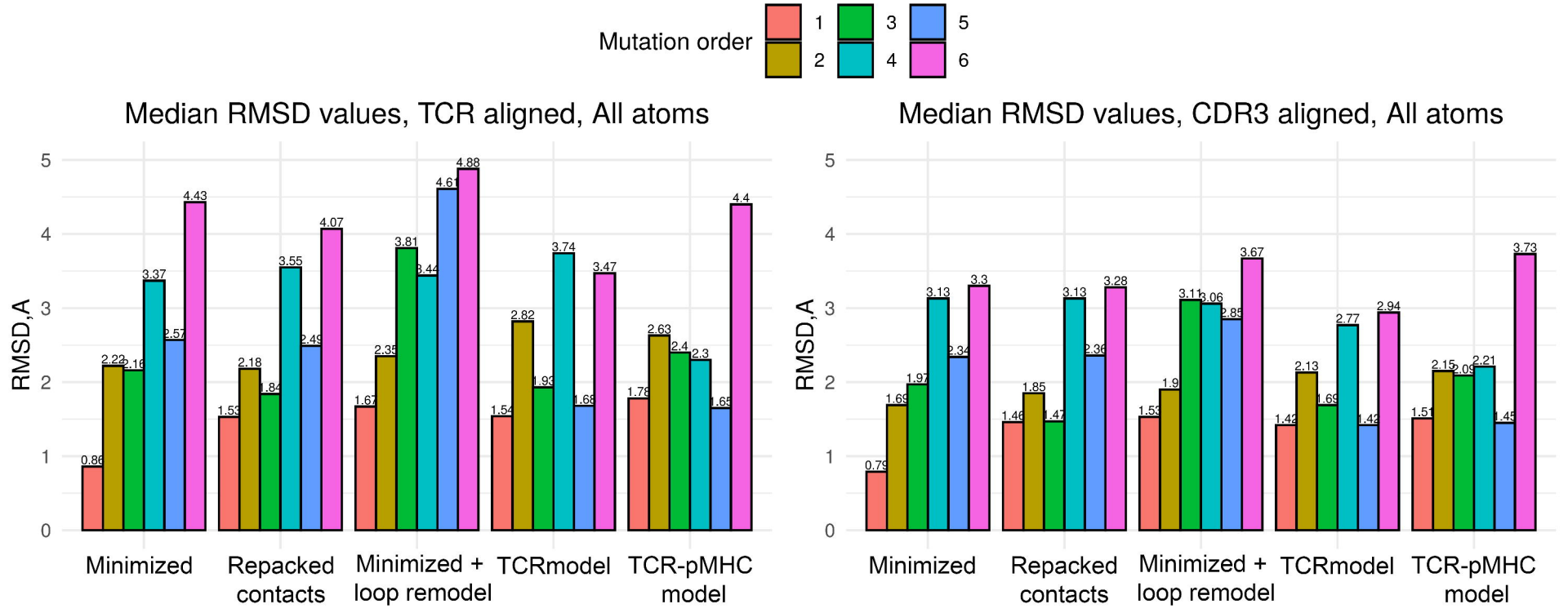
Mutation order
1
2
3
4
5
6
Median RMSD values, TCR aligned, All atoms
RMSD,A
0
1
2
3
4
5
0.86
2.22
2.16
3.37
2.57
4.43
1.53
2.18
1.84
3.55
2.49
4.07
1.67
2.35
3.81
3.44
4.61
4.88
1.54
2.82
1.93
3.74
1.68
3.47
1.78
2.63
2.4
2.3
1.65
4.4
Minimized
Repacked contacts
Minimized + loop remodel
TCRmodel
TCR-pMHC model
Median RMSD values, CDR3 aligned, All atoms
RMSD,A
0
1
2
3
4
5
0.79
1.69
1.97
3.13
2.34
3.3
1.46
1.85
1.47
3.13
2.36
3.28
1.53
1.9
3.11
3.06
2.85
3.67
1.42
2.13
1.69
2.77
1.42
2.94
1.51
2.15
2.09
2.21
1.45
3.73
Minimized
Repacked contacts
Minimized + loop remodel
TCRmodel
TCR-pMHC model